

**POWER PERFORMANCE INVESTIGATION AND CONTROL SYSTEM
DESIGN OF GRID-CONNECTED SMALL WIND TURBINES**

By

Md Alimuzzaman

A thesis submitted to the

School of Graduate Studies

in partial fulfillment of the requirements for the degree of

MASTER OF ENGINEERING

Faculty of Engineering and Applied Science

Memorial University of Newfoundland

May, 2013

St. John's

Newfoundland

ABSTRACT

In this research, the power performance of three grid-connected small wind was investigated. Two small wind turbines were tested in a number of load conditions and test data were collected for approximately two months. Data was analyzed for active power, power factor and reactive power. Results indicate that the type of local load does not significantly affect the power curve of a small wind turbine. It was also observed that above 15% of rated power, the power factor of a grid-connected small wind turbine was almost constant.

In the second stage of this research, another small vertical axis wind turbine was tested and data was analyzed. A maximum power point tracking (MPPT) table for optimal operation of a small vertical axis wind turbine was derived mathematically and verified by simulation model. The derived MPPT table was programmed in an inverter; the wind turbine was tested and data was logged for more than three months. The power curve from the logged data was produced and compared with the manufacturer's power curves of the turbine.

At the last stage of this research, a Matlab simulation model of a grid-connected 1.1 kW wind turbine system was developed along with active and reactive power control system. The supplied reactive power from the wind turbine was controlled by changing the phase angle of Pulse Width Modulation (PWM) in the wind turbine inverter. A proportional controller was used to maintain the reactive power supplied by the wind turbine. On the other hand, a PI controller was used to maintain the wind turbine operation at an optimum tip speed ratio to extract maximum power from the wind. The simulation results confirm

that the designed system is able to control the wind turbine and capable of providing the required reactive power.

ACKNOWLEDGEMENTS

First, the author would like to express profound gratitude to his supervisor, Dr. M. Tariq Iqbal, for his supervision, motivation, immense knowledge, encouragement, scientific reviewing and valuable suggestions throughout the research work. His moral support and guidance enabled the author to complete the research successfully.

The research received funding from Natural Science and Engineering Research Council (NSERC), Wind Energy Strategic Network (WESNet) and School of Graduate Studies (SGS) of Memorial University. The author likes to gratefully acknowledge the financial support provided by those organizations.

The author also would like to thank Wind Energy Institute of Canada (WEICan) for providing technical support for the experiments. The author likes to mention the names of Gerald Geroux and Andy Doucette from WEICan and Heather Davis from Sugan Research for their assistance.

At last but not least author likes to thank his wife Tania Sarmin Sultana for her ceaseless mental support. Author would like to express his gratitude to his parents and siblings for their support and encouragement.

Table of Contents

ABSTRACT	ii
ACKNOWLEDGEMENTS	iv
Table of Contents.....	v
List of Tables.....	viii
List of Figures	ix
List of Symbols.....	xii
List of Abbreviations	xiv
Chapter 1 INTRODUCTION	1
1.1 Background.....	1
1.2 Related Works	2
1.3 Research Motivation and Objectives.....	6
1.4 Thesis Organization.....	7
Chapter 2 INVESTIGATION OF POWER OUTPUT OF TWO SMALL WIND TURBINES.....	9
2.1 Introduction	9
2.2 Grid-connected Small Wind Turbines.....	10
2.3 Data Analysis Procedure	11
2.3.1 IEC-61400-12-1 standard	12
2.3.2 Bins method.....	13
2.4 Experiments and Results	14
2.4.1 Experiments with turbine A.....	14

2.4.1.1 Power Performance without any Local Load	15
2.4.1.2 Experiment with Heaters	17
2.4.1.3 Experiment with a 5hp Induction Motor	19
2.4.2 Experiments with Turbine B.....	23
2.4.2.1 Power performance without any Local Load	23
2.4.2.2 Experiment with Heaters	25
2.4.2.3 Experiment with 5hp Induction Motor and Capacitors	27
2.5 Conclusion.....	31
Chapter 3 DATA LOGGING AND POWER OPTIMIZATION OF A NOVEL VERTICAL AXIS WIND TURBINE	32
3.1 Introduction	32
3.2 Technical information of the turbine and generator	33
3.3 Block diagram of the system	35
3.4 Power curve determination from the available turbine data.....	36
3.5 Gearbox Ratio Analysis.....	37
3.6 Determination of a Maximum Power Point Tracking (MPPT) Table	40
3.6.1 Power calculation for the MPPT table.....	40
3.6.2 Efficiency of the generator, rectifier and inverter	41
3.6.3 DC Voltage of the MPPT table.....	42
3.6.4 MPPT table	45
3.7 Dynamic Modeling and Simulation.....	47
3.8 Data Analysis.....	49

3.9 Summary.....	52
Chapter 4 Control System Design for Active and Reactive Power Control of a Small Grid Connected Wind Turbine	54
4.1 Introduction	54
4.2 Some Small Wind Turbines Issues	55
4.3 Small Wind Turbine Configuration for this Research.....	55
4.4 System Modeling.....	56
4.5 Control System Design.....	59
4.5.1 Active Power Control System	59
4.5.2 Reactive Power Control System	61
4.6 System Simulation and Results	63
4.6.1 Case study one	63
4.6.2 Case study two.....	64
4.6.2 Case study three.....	65
4.7 Summary.....	66
Chapter 5 CONCLUSION AND RECOMMENDATIONS	67
5.1 Summary of the Research.....	67
5.2 Recommendations for Future Work	69
Bibliography.....	70
Appendix A Data Analysis procedure using the developed Macro.....	80
Appendix B Values of Simulation Block Parameters for Chapter Four.....	86
Appendix C List of Research paper.....	87

List of Tables

Table 3.1: Turbine optimum rotation and maximum power data from the manufacturer .	34
Table 3.2: Generator information obtained from the generator manufacturer	35
Table 3.3: Tip speed ratio calculation	38
Table 3.4: Calculated output power of the inverter	42
Table 3.5: Optimum rotation of turbine and generator.....	43
Table 3.6: Optimum rotational speed vs. DC Voltage	44
Table 3.7: Input DC voltage and output power of the inverter.....	45
Table 3.8: MPPT table_ derived.....	46
Table 3.9: Calculated and Simulated Data Comparison.....	49
Table B-1: Values of Simulation Block Parameters for Chapter Four.....	86

List of Figures

Figure 2.1: Block diagram of a small wind turbine	10
Figure 2.2: Block Diagram of an Experimental Setup	12
Figure 2.3: Power performance of turbine A without any local load a) power curve, b) power factor, c) reactive power	16
Figure 2.4: Block diagram for an experimental setup with resistive load (heater)	17
Figure 2.5: Power performance comparison of turbine A with resistive load a) power curve, b) power factor and c) reactive power	19
Figure 2.6: Block diagram for experimental setup with an inductive load (motor) and capacitor.....	20
Figure 2.7: Power factor comparison of the whole building with inductive and capacitive load	21
Figure 2.8: Reactive power comparison of the whole building with inductive and capacitive load	21
Figure 2.9: Power performance comparison of turbine A with inductive and capacitive load a) power curve and b) power factor, c) reactive power	22
Figure 2.10: Power curve variation for turbine B under the similar conditions.....	23
Figure 2.11: Power performance of turbine B without any local load a) power curve, b) power factor and c) reactive power	25
Figure 2.12: Block diagram for experiment setup with resistive load (heater) for turbine B	26

Figure 2.13: Power performance comparison of turbine B with resistive load a) power curve, b) power factor and c) reactive power	27
Figure 2.14: Block diagram for the experimental setup with an inductive load (motor) and capacitors for turbine B	28
Figure 2.15: Power factor comparison of the whole building with inductive and capacitive load connected to turbine B	29
Figure 2.16: Reactive power comparison of the whole building with inductive and capacitive load connected to turbine B	29
Figure 2.17: Power performance comparison of turbine B with inductive and capacitive load a) power curve, b) power factor and c) reactive power	30
Figure 3.1: Vertical Axis Wind Turbine of this research	33
Figure 3.2: Block diagram of the wind turbine system	36
Figure 3.3: Initial power curve of the wind turbine and the manufacturer provided power curve	37
Figure 3.4 : Generator power vs. rpm.....	39
Figure 3.5: System block diagram indicating the use of MPPT table	40
Figure 3.6: Generator efficiency including rectifier efficiency as a function of power. ...	41
Figure 3.7: Inverter efficiency	41
Figure 3.8: DC voltage vs. Generator rpm	43
Figure 3.9: MPPT curve programmed in the inverter	46
Figure 3.10: Simulation model of the VAWT	48

Figure 3.11: (a) MPPT_derived and old MPPT curves (b) Power performance with old MPPT and MPPT_derived.....	50
Figure 3.12: Four MPPT tables tested on the system.....	51
Figure 3.13: Out power comparison with different MPPT tables.....	52
Figure 4.1: Block diagram of a small wind turbine system.....	56
Figure 4.2: Wind turbine model.....	57
Figure 4.3: System modeling in Simulink.....	59
Figure 4.4: Flow chart for active power control.....	61
Figure 4.5: Reference signal, carrier signal and gate pulse for PWM.....	62
Figure 4.6: Case study one.....	63
Figure 4.7: Case study two.....	64
Figure 4.8: Case study three.....	65
Figure A-1: Macro Scheduler record tab.....	81
Figure A-2:Macro Scheduler file name.....	81
Figure A-3: command file call.....	82
Figure A-4: Command file on PC (OS windows).....	82
Figure A-5: Folder select command window.....	83
Figure A-6: Command to combined multiply files.....	83
Figure A-7: Developer tab on Microsoft Excel.....	84

List of Symbols

A	=	Rotor blade area
$B_{10\text{min}}$	=	10 min average air pressure
C_p	=	Power coefficient
i_q, i_d	=	q and d axis current
L_q, L_d	=	q and d axis inductances
N_i	=	Number of 10 min data sets in bin i
p	=	Pole pairs number
$P_{10\text{min}}$	=	Measured power averaged over 10 min
P_i	=	Normalized and averaged power in bin i
P_{max}	=	Maximum power produced for optimum rotation of the blades.
P_n	=	Normalized power output
$P_{n, i, j}$	=	Normalized power of data set j in bin i
r	=	blade radius
R	=	Resistance of the stator windings
R_0	=	Gas constant of dry air
$T_{10\text{min}}$	=	10 min averaged absolute air temperature
T_e	=	Electromagnetic torque
V	=	Wind speed
$V_{10\text{min}}$	=	10 min averaged wind speed

- V_i = Normalized and averaged wind speed in bin i
- V_n = Normalized wind speed
- $V_{n, i, j}$ = Normalized wind speed of data set j in bin i
- V_q, V_d = q and d axis voltage
- W_{opt} = Optimum rotation of the blades
- λ = Tip speed ratio
- λ_a = Amplitude of the flux
- ρ_{10min} = 10 min averaged air density
- ρ_o = Reference air density
- ρ = Air density
- ω = Rotor blade rotation
- ω_r = Angular velocity of the rotor

List of Abbreviations

AC	=	Alternating Current
ANN	=	Artificial Neural Network
CSBI	=	Current Source Boost Inverter
DC	=	Direct Current
DFIG	=	Doubly-Fed Induction Generators
HAWT	=	Horizontal Axis Small Wind Turbine
IEC	=	International Electrotechnical Commission
ISO	=	International Organization for Standardization
MPPT	=	Maximum Power Point Track
NSERC	=	Natural Science and Engineering Research Council
PEI	=	Prince Edward Island
PI	=	Proportional Integral
PMG	=	Permanent Magnet Generators
PPWM	=	Phasor Pulse-Width-Modulation
PSF	=	Power Signal Feedback
PWM	=	Pulse Width Modulation
STATCOM	=	Static Synchronous Compensator
SVC	=	Static Var Compensator
THD	=	Total Harmonic Distortion

TSR = Tip Speed Ratio

VAWT = Vertical Axis Small Wind Turbine

WECS = Wind Energy Conversion System

WEICan = Wind Energy Institute of Canada

Chapter 1

INTRODUCTION

1.1 Background

Global Energy demand is increasing day by day. The World's Electricity demand grows almost twice as fast as its total energy consumption. Assuming the recent rapid expansion of wind, solar and hydro power, by 2035, renewable industries can account for almost one-third of total electricity output [1].

Wind turbine generation has been contributing a remarkable percentage to the total power generation in the world. Recently, it has been increasing radically because of governments support and public environmental concerns [2]. According to British petroleum statistical review of world energy June, 2012, worldwide wind energy production has increased by more than 25.8% in 2011 from 2010. Wind power has contributed about 194.8 million tones oil equivalent energy in 2011 [3].

Small wind turbines are becoming popular gradually. Grid-connected small wind turbines are very useful where both the grid and the wind energy are available. People are more interested in small wind turbine after the net-metering regulations. In net-metering system, if the wind turbine is grid-connected and if there is excess wind power then wind turbine system can use the grid to store excess power. On the other hand, users can get power from grid when there is a lack of power production from the wind. In grid-connected wind turbine and net metering situation, there is no need for battery backup or

any other type of backup system as the grid can be used as storage. This advantage also reduces the initial cost for small wind turbine.

As the uses of small wind turbines are increasing day by day, it is an urgent demand to focus on commercially available grid-connected small wind turbine behaviour under variable electrical load conditions. More research should take place on grid-connected small wind turbine power performance, maximum power extraction and their control system.

1.2 Related Works

Wind turbines are divided into two main groups. One is horizontal axis wind turbine (HAWT) and another one is vertical axis wind turbine (VAWT). HAWT has its main rotor and generator at the top of its tower whereas VAWT has its rotor shaft perpendicular to ground and its structure is relatively simple [4]. VAWT has low efficiencies compared with HAWT. For that reason, HAWT are more popular than VAWT. However VAWT is suitable where wind speed is low [5]. For low rotational speed, VAWT are quieter than HAWT. Therefore, VAWT are appropriate for the applications which are close to population centers.

To produce electric energy, doubly-fed induction generators (DFIG) in large wind turbines and permanent magnet generators (PMG) in small wind turbines are widely used. Since a PMG has its own permanent magnet, it does not require an external excitation current and it does not consume reactive power from the grid. Additionally PMG has high efficiency and a small size compared to a DFIG. That is why PMG are dominant in small wind turbine systems [6][7] [8].

Wind turbine power generation depends on wind speed. As the wind speed changes every moment, the output of generator is wild AC. In order to make the power usable, the output of the generator is connected to a rectifier. The rectifier output is DC and to control the DC power various type of control topology are in use. A semi controlled rectifier is proposed in article [9]. Another fully controlled rectifier for wind energy conversion system (WECS) is projected in [10]. Besides, another simple way is to add another dc-dc converter after the rectifier. There are three main types of dc-dc converter-buck, boost and buck-boost converter. Among them boost converter is most frequently used in WECS [11][12][13][14][15]. The output DC power is connected to an inverter. The inverter output is AC power. The inverters are configured to produce sine wave output. They are also built up in such a way that they produce grid frequency and also maintain grid voltage [16]. The standard IEC-61400-21 (International Electrotechnical Commission) states the power quality issue for wind turbine. The main concerns of power quality are voltage fluctuation and dips, reactive power and harmonics. Paper [17] describes the grid power quality for variable speed wind turbine.

In wind turbine industry, various types of control systems are available. For over speed control and mechanical power control furling, flapping, passive pitching, and soft stall are mostly used [18][19]. Among them furling and soft stall are simple and inexpensive control mechanisms for small wind turbines [20].

A Wind turbine can extract maximum power from wind if the rotor blades run at such a speed that it can maintain an optimum tip speed ratio (TSR). TSR is the ratio between the rotational speed of wind turbine blade and the wind speed. As the wind turbine characteristics are nonlinear, a proper control system is needed to extract maximum

power from wind [21][22]. Many research works and implementations are available regarding maximum power point track (MPPT) system. All the available techniques can be divided into three main categories, and they are, a) Tip speed ratio control (TSR) b) Perturbation and observation or hill climbing searching c) power signal feedback (PSF)[22][23].

In the TSR methodology, the rotor speed and the wind speed are measured at every moment and the TSR is calculated. The control system will take action (adjust the generator load) to maintain an optimum TSR[24] [25][26][27][28] [29]. In article[24] [25], a fuzzy logic controller has been used to track the maximum power point. In article [27], [28] and [29]an artificial neural network (ANN) has been used to estimate wind speed and the estimated wind speed and the optimum TSR value are used to calculate rotor speed command value. This methodology is useful because it replaces the anemometer.

For hill climbing searching methodology, the controller adjusts the load to increase or decrease the rotor speed and measures the following power to take decision for the next step. Some hill climbing searching methodologies have constant step [30] [31] and some other have variable step [32]. An adaptive control algorithm has been introduced in [33] for MPPT. In this technique the control system automatically changes its hill climbing searching method by using estimation process and adaptive memory.

For PSF methodology, maximum power is tracked by using measured current power and a look up table [22]. The main challenge of this technique is to develop a proper look up table for a particular wind turbine. A look up table can be developed by computer simulation or experimental test. Turbine equation can be used to find out reference power

for PSF based MPPT control [34]. Fuzzy logic control based PSF is discussed in the paper [35][36].

Most commercially available small wind turbines have permanent magnet generator. So the system does not consume reactive power from grid but wind turbine generation can be used to provide local reactive power consumption. It will minimize reactive power flow over the grid and thus it will minimize the losses [37]. In article [37], a stochastic optimization methodology has been introduced to control reactive power of wind turbines. Reactive power of wind turbine generation system depends on the inverter configuration. There are extensive researches concerning the reactive power control of the inverter. In [38], a fuzzy logic controller has been used to control both active and reactive power. In [39], a predictive control method has been introduced to control both active and reactive power. A nonlinear sliding mode control system for power control of a three phase grid-connected inverter is discussed in [40]. A non linear decoupling method based reactive power control methodology is proposed for grid-connected PV inverter in [41]. A controlling strategy for Current Source Boost Inverter (CSBI) using phasor pulse-width-modulation (PPWM) is proposed and verified using simulation result in [42]. Article [43] describes only the reactive power control with a CSBI using PPWM in details with both simulation results and experimental results. All the techniques are applied to grid-connected inverter. The inverter can be controlled to provide reactive power to the grid. In most cases, the techniques are applied and verified with a simple DC input to the inverter. A research should be performed on a grid connected small wind turbine system along with inverter that can control reactive power flow.

1.3 Research Motivation and Objectives

Small wind turbines are generally used to meet small community energy demand and remote power generation. The local load connected to these turbines can be resistive, inductive or capacitive. Commercially available small wind turbine manufacturers provide a power curve for a particular wind turbine along with all the specification. Wind turbine test organization further verifies the power curve by logging practical data. Generally when the data is collected to produce a power curve, the wind turbine is directly connected to the grid. There may be some load present between the turbine and the grid but in most of the cases the load is resistive (light, heater of the turbine shed). Research is urgently needed to examine the small wind turbine power performance when various types of local loads are connected between the turbine and the grid. This has not been reported in the literature. Investigation of grid-connected small wind turbine's power performance under resistive, inductive and capacitive load is the first objective of this research.

Grid tied inverter with look up table based MPPT controller is the most simple, reliable and commonly used inverter in commercially available inverters for small wind turbine market. The main challenge of this technology is to create a perfect MPPT look up table for a particular turbine. No well-defined method is reported in literature. The next objective of this research is to build up a simulation model of a small wind turbine with all practical parameter and thus develop a power curve and a MPPT table for PSF based MPPT controller.

In this day and age, reactive power of small wind turbine is an important issue. Various types of technique are available for controlling reactive power flow of a grid tie inverter.

However research on reactive power control for grid-connected small wind turbine has a very shadowy existence and little reported in the literature. The final objective of this thesis is to develop a simulation model of a grid-connected small wind turbine along with a reactive power control system.

1.4 Thesis Organization

In chapter two, the experiments of two small wind turbines with resistive, inductive and capacitive load are described in details. The data collection procedure and the analysis method are also presented in this chapter. The logged data are analyzed and plotted for active, power factor and reactive power. Power curves of these turbines are plotted with load and without any load connected between the wind turbine and the grid following the standard IEC-61400-12-1. Power performances of two small turbines are compared for different types of loads condition.

In chapter three, a novel vertical axis wind turbine system is analyzed. A MPPT table has been derived mathematically with the help of available manufacturer provided data. A simulation model of the system has been built up with a MPPT controller based on tip speed ratio control. The mathematically derived MPPT table is verified with the simulation model. The MPPT table was installed in turbine's inverter and data was collected and from the logged data, turbine power curve was generated. At the end of this chapter, power curves generated with various inverter configurations (different MPPT) are compared.

In chapter four, a control system has been developed that allows wind turbine to provide reactive power to the local load connected between the grid and the wind turbine.

Detailed discussion of active and reactive power control methodology are presented in this chapter. The proposed system along with all sub-systems has been modeled and simulated in Matlab/Simulink. Simulation results for three different cases are also shown in this chapter.

In conclusion, the summary of the work, contribution and achievements of the research are presented in chapter five. Some recommendations for future works are also included in the chapter.

Chapter 2

INVESTIGATION OF POWER OUTPUT OF TWO SMALL WIND TURBINES

2.1 Introduction

The wind industry contributes a significant percentage of electric power generation all over the world. The power performance and power quality of wind turbines and their interaction with the grid is becoming an important issue [44]. Small wind turbines are being widely used to fulfill local demands. They are used to power dairy farms, water supplies for small communities, small industry, irrigation and greenhouses. Many of these turbines are grid-connected, therefore when there is excess electricity they can supply the extra power to a grid and when there is a lack of electric power from the wind turbine, the system can use power from the grid assuming net-metering is available.

Power performance investigation of small wind turbines is very important. Manufacturers provide a power curve for their wind turbines, which is essentially turbine-produced active power versus wind speed. Depending upon the situation, the small wind turbine load may be resistive, inductive or sometimes capacitive in nature. So, besides active power, reactive power performance and power factor condition under variable electric load configurations are also needed to study.

Wind Energy Institute of Canada (WEICan) is an institute where small wind turbines are tested for verifying their power curves. WEICan suggested to test small wind turbine to investigate whether these turbines can provide their stated power under different types of

loads or not. To investigate this issue, two turbines were selected for experiments and they are called turbine A and turbine B below. The identity of these two turbines is being kept confidential in this thesis to protect commercial interests of turbines manufacturers.

In this chapter, the power performance of two small wind turbines is investigated. Two wind turbines are tested at the WEICan with a resistive, inductive and capacitive load. Recorded data are compared and analyzed for active power, reactive power and power factor. The results and discussion are presented below.

2.2 Grid-connected Small Wind Turbines

Figure 2.1 represents a typical small wind turbine system. Most small wind turbine systems consist of a rotor, generator, rectifier and inverter. After an inverter, the system is connected to an AC panel; the local load is also connected to an AC panel. Before connection to the grid, typically, power goes through a transformer to change the voltage level.

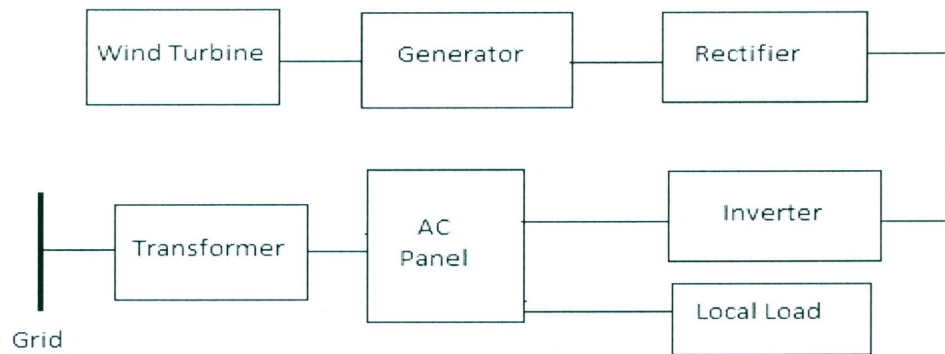


Figure 2.1: Block diagram of a small wind turbine

For our experiments, the system was arranged in a similar way. To convert the wind energy into mechanical energy, a wind rotor is used. For electric power generation,

various types of generators have been used. Among them, a permanent magnet generator is widely used as mentioned previously. As the wind speed and wind direction change every second, so does the total extracted wind power. As a result, the produced electric power from the generator is not uniform. The AC power from the generator is first converted to DC power with the help of a rectifier. Then, the DC power is again converted to the desired AC power so that the output can be connected to the grid. The inverter plays a vital role in this system. The inverters must produce high quality sine-wave output and must follow the frequency and voltage of the grid. The inverter must observe the phase of the grid, and the inverter output must be controlled for voltage and frequency variations [16]. Most of the commercially available grid tie inverters have an active power factor controller to reduce the Total Harmonic Distortion (THD).

2.3 Data Analysis Procedure

For each wind turbine used in the experiments, there is a meteorological mast assigned to measure the wind speed and wind direction. The mast was located according to IEC-61400-12-1 standard [45]. The power was measured using a power measurement device based on current and voltage measurement on each phase. The power measurement device was located between the turbine and the grid so that it can measure only the net active power. The wind turbines were connected to the loads before connection to the grid. Here in these experiments, this type of load is called local load. Two transducers were used for data logging. One transducer was connected between the wind turbine and the local load. Another transducer was connected between the local load and the grid. The first transducer measured how much active and reactive power was being produced by the

turbine and it also measured its power factor. The other transducer measured how much active or reactive power exchanges occurred with the grid. A block diagram of the experimental setup is shown in Figure 2.2.

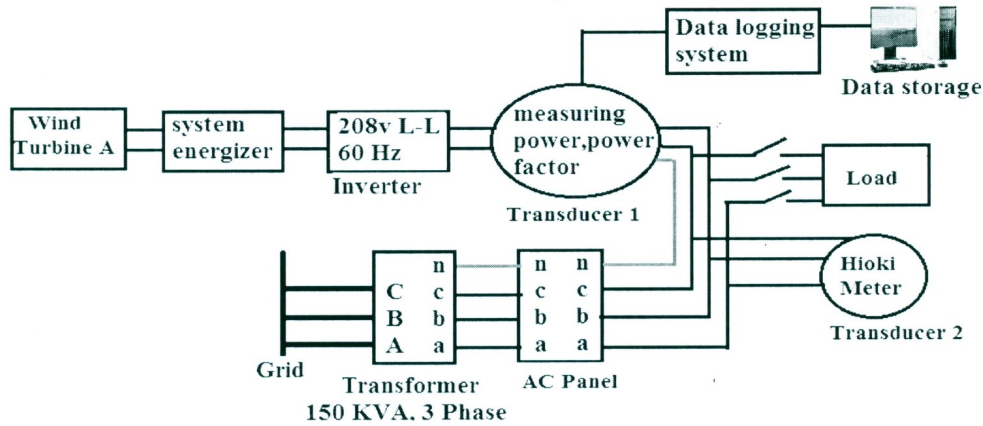


Figure 2.2: Block Diagram of an Experimental Setup

Data was collected at one second interval. The collected data was first normalized and then stored using the bins method [46]. The wind speed ranges are divided into 0.5m/s contiguous bins centered on multiple of 0.5m/s

2.3.1 IEC-61400-12-1 standard

All the collected data has been normalized according to IEC-61400-12-1 standard. For normalization two air densities are used as reference. One is ISO standard atmosphere (1.225 Kg/m³) and another one is measured on the site.

The measured air density on the site is represented by the equation below.

$$\rho_{10\min} = \frac{B_{10\min}}{R_0 T_{10\min}} \quad (2.1)$$

$\rho_{10\min}$ = 10 min average air density

$T_{10\min}$ = 10 min average absolute air temperature

$B_{10\min}$ = 10 min average air pressure

R_0 = Gas constant of dry air 28705 J/(Kg*K)

According to IEC-61400-12-1 standard, the measured power produced by the wind turbine and the wind speed are represented by the following equations.

$$P_n = P_{10\min} \frac{\rho_o}{\rho_{10\min}} \quad (2.2)$$

P_n = Normalized power output

$P_{10\min}$ = Measured Power average over 10min

ρ_o = Reference air density

$$V_n = V_{10\min} \left(\frac{\rho_{10\min}}{\rho_o} \right)^{1/3} \quad (2.3)$$

V_n = Normalized wind speed

$V_{10\min}$ = 10 min average wind speed

2.3.2 Bins method

For the power curve, bins method was applied to normalize the power and wind speed.

For this purpose, 0.5m/s bins was used and the following two equations are used to calculate the mean values of the normalized wind speed and normalized power output.

$$V_i = \frac{1}{N_i} \sum_{j=1}^{N_i} V_{n,i,j} \quad (2.4)$$

$$P_i = \frac{1}{N_i} \sum_{j=1}^{N_i} P_{n,i,j} \quad (2.5)$$

V_i = Normalized and average wind speed in bin i ;

$V_{n, i,j}$ = Normalized wind speed of data set j in bin i;

P_i = Normalized and average power in bin i ;

$P_{n,i,j}$ = Normalized power of data set j in bin i ;

N_i = Number of 10 min data sets in bin i ;

2.4 Experiments and Results

To investigate the power performance of small wind turbines, two different turbines were used. For our experiment, the turbines are referred to as turbine A and turbine B. Both the turbines have PMG. Turbine A is a 1.1 KW small wind turbine and it uses stall regulation for its control system. Turbine B is a 1.3 KW small wind turbine and it uses furling method for its control system. Normalized data is used in this chapter to hide the wind turbine identity.

For data logging, a Campbell scientific 1000 data logger was used to collect the data for every second interval and stored in a PC. This creates a file for every day (24 hours). This raw data (second data) was later converted to ten minute average data. Then, this ten minute data was normalized and the power curve was plotted using the bins method. The bins method was also used to compare the reactive power and power factor.

For the experiment with a motor, a second transducer (Hioki meter) was used. It can measure three phases - active power, power factor and reactive power for one second interval and store the data in a memory card. Later, this collected data can be easily moved from the memory card to a PC.

2.4.1 Experiments with turbine A

The specifications of turbine A are as follows:

Rated Power: 1.1 KW

Rated wind speed: 12.5 m/s
 Power Regulation: Non-stop output control
 Maximum Power: 4 kW
 Permanent magnet generator (3 phase, synchronous)
 Over Speed Control/Protection: Stall Regulation
 Inverter output Voltage: 120V/208V
 Voltage Tolerance: $\pm 5\%$
 Grid Frequency: 60Hz
 Frequency Tolerance: $\pm 0.00083\%$

2.4.1.1 Power Performance without any Local Load

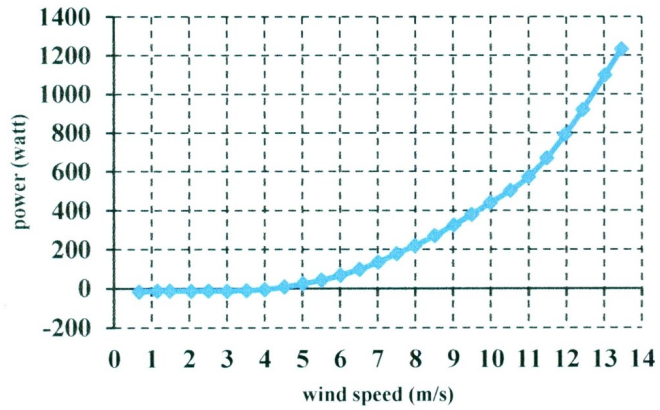
The turbine was grid-connected. For comparison with local load and without local load, the power performance data of the turbine without any local load was collected for ten days. Then, ten minute average value of data was calculated and then it was normalized. Finally, by using the bins method, the power curve, reactive power curve and power factor curve were plotted.

Figure 2.3(a) shows the power curve of the wind turbine. In Figure 2.3(b), the power factor is plotted and it indicates that when wind speed is more than 9 m/s, the power factor is close to unity.

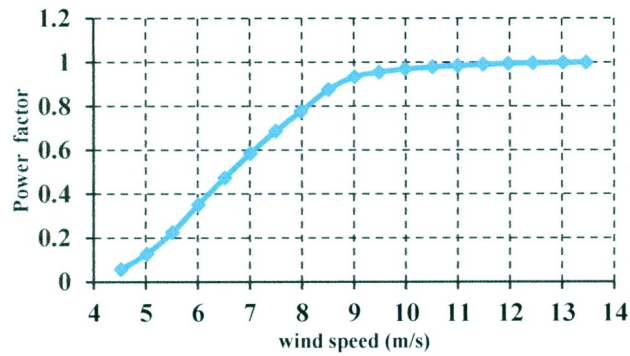
$$\text{Power factor} = \text{active power} / \text{apparent power} \quad (2.6)$$

$$\text{Apparent power}^2 = \text{active power}^2 + \text{reactive power}^2 \quad (2.7)$$

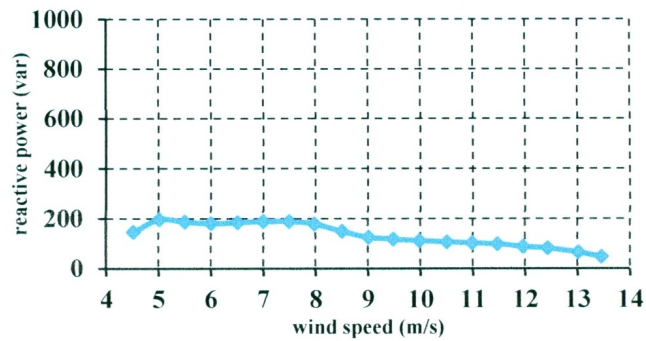
Reactive power is plotted in Figure 2.3(c) and it can be observed that there is negligible change of reactive power with wind speed changes and reactive power is always less than 200 var.



(a)



(b)



(c)

Figure 2.3: Power performance of turbine A without any local load a) power curve, b) power factor, c) reactive power

Active power output depends on wind speed and it typically increases as the wind speed increases. But with wind speed increase, there is no significant change in reactive power

compared to active power change. So, at high wind speed, as the active power is much higher than the reactive power, apparent power is almost equal to the active power and thus the power factor improves at high wind speed.

2.4.1.2 Experiment with Heaters

To test whether resistive load can have an effect on the power performance of wind turbines, three heaters were connected, as shown below in Figure 2.4. It is noted that the turbine is connected to phase b and phase c of the transformer and here phase to phase voltage is 208V and phase to neutral voltage is 120V. The heaters were adjusted to maximum point. One of the heaters was a turbine shed heater. It was configured for 208V and it was connected to phase b and phase c. The other heaters were portable and configured for 120V. One of them was connected to phase b and neutral, and another one is connected to phase c and neutral. They were kept outside the shed to prevent overheating.

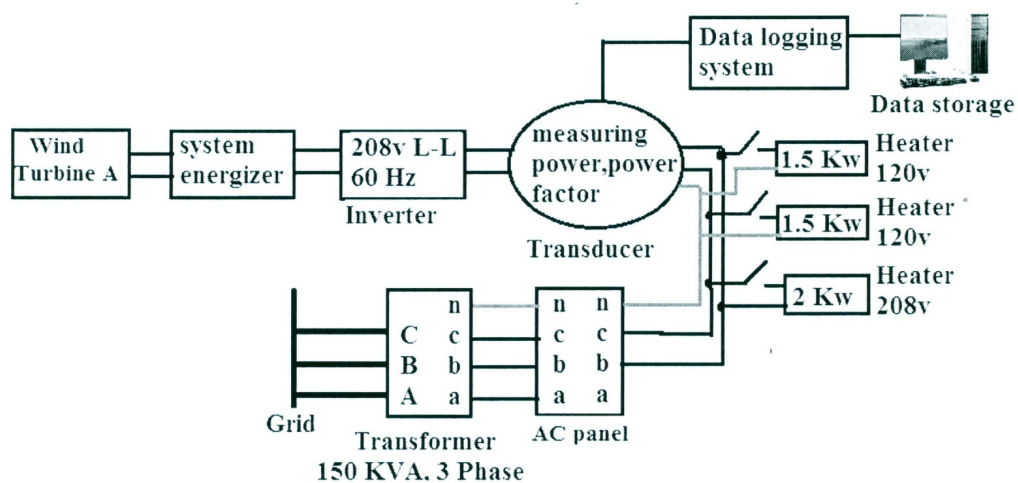
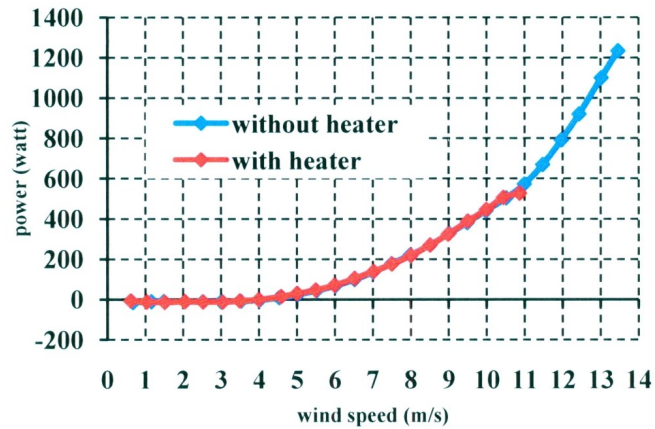
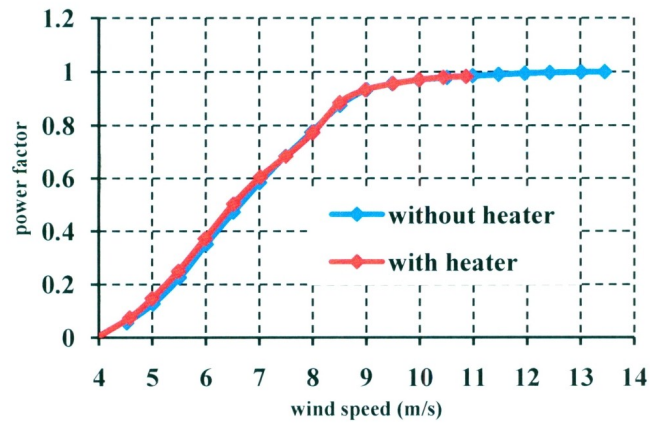


Figure 2.4: Block diagram for an experimental setup with resistive load (heater)

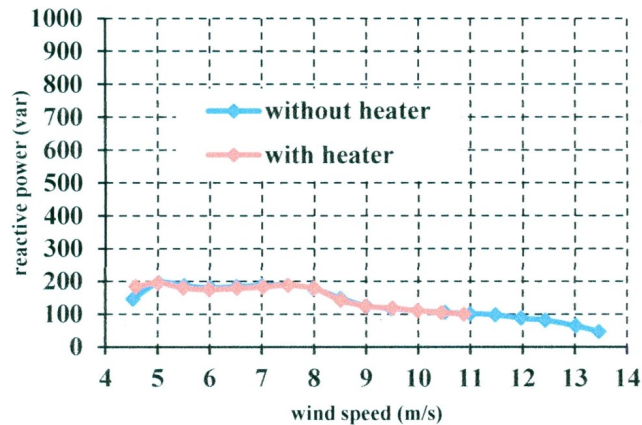
Heaters were connected for six days and one second data was collected. Data was converted to ten minute average data and after that the data was normalized. Using the bins method, the power performance curves were plotted and these are shown in Figure 2.5. It is noted that during the experiment with heaters, maximum wind speed was 11 m/s.



(a)



(b)



(c)

Figure 2.5: Power performance comparison of turbine A with resistive load a) power curve, b) power factor and c) reactive power

From Figure 2.5(a), it can be seen that there is no change in power curve. In Figure 2.5(b), there is no change in power factor also. In both cases (with and without heater), when wind speed is greater than 9 m/s power factor was very close to unity. Figure 2.5(c) shows that there is no significant change in reactive power. In both cases, reactive power decreases gradually and it is always less than 200 var. Therefore, we can say that there is no significant effect of heaters on the output power, power factor and reactive power.

2.4.1.3 Experiment with a 5hp Induction Motor

For the experiment with an inductive load, a 5hp induction motor was used as load. The motor was connected before the transformer. The motor was in no-load mode, so its active power consumption was low but reactive power was high. The motor was a three phase motor. The motor was left connected for three days and one second data was collected for those days. At no load condition, the motor required 1.735kvar. The value of

the compensation capacitors was calculated to provide required reactive power to the motor and its value was $35\mu\text{F}$ for each phase to phase connection. Practically $34.37\mu\text{F}$, 208V capacitors were available and they were connected for each phase to phase connection for two more days and one second data was collected again. Data was analyzed using the procedure mentioned earlier.

In this case, another transducer (Hioki meter) was connected before the transformer. That meter measured the whole building power performance for every second. Here, the building includes the wind turbine, induction motor, data logger, and building lights. Data was analyzed using the bins method. The connection diagram is shown in Figure 2.6.

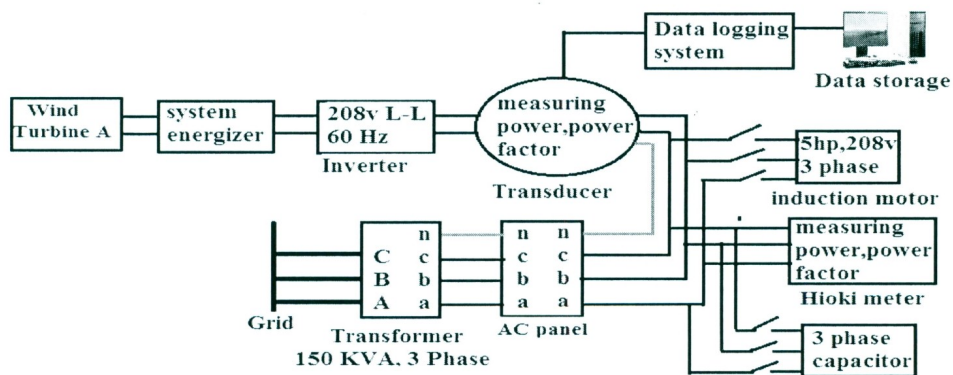


Figure 2.6: Block diagram for experimental setup with an inductive load (motor) and capacitor

Experimental results and comparison are shown in Figures 2.7 & 2.8. From Figure 2.7, we can find that, when the inductive load was connected, the whole building power factor decreased and when compensation capacitors were connected, the power factor improved. Figure 2.8 shows that the total demand of reactive power for the whole building was more than 1600var, but with compensation capacitors it was similar to reactive power without a motor.

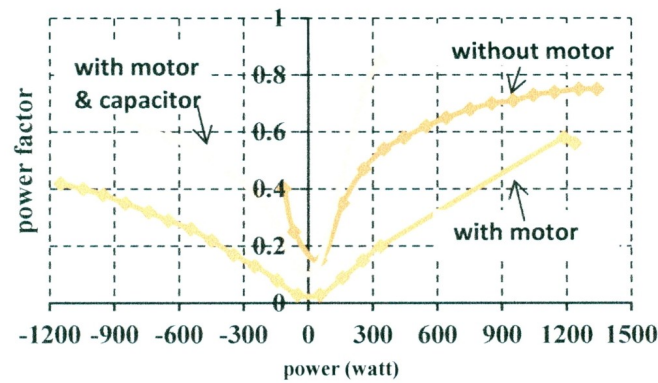


Figure 2.7: Power factor comparison of the whole building with inductive and capacitive load

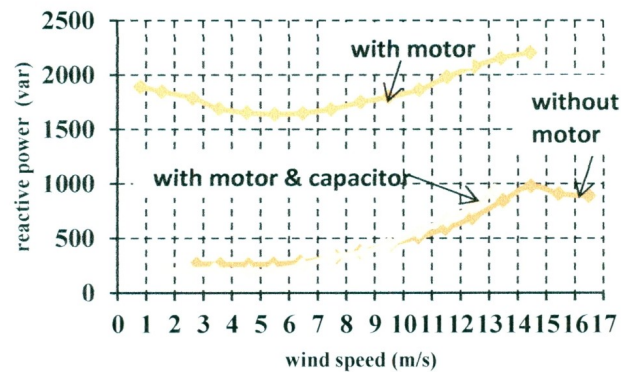
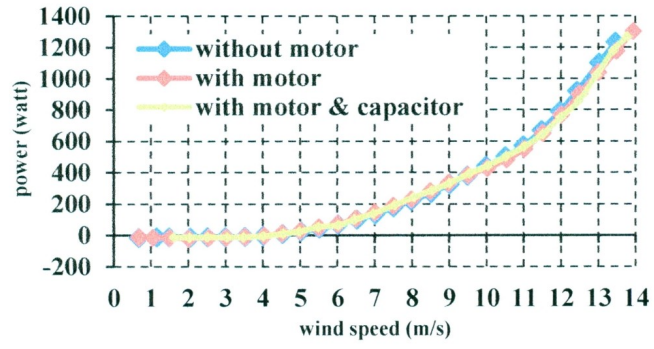
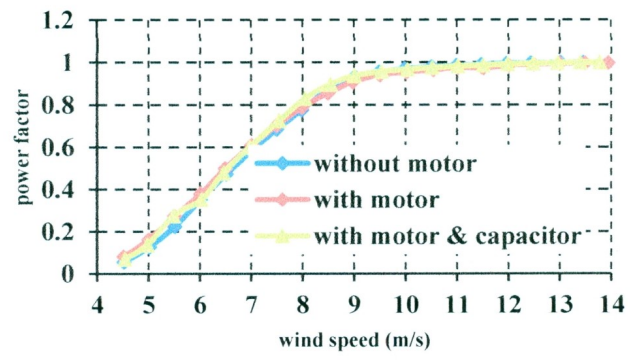


Figure 2.8: Reactive power comparison of the whole building with inductive and capacitive load

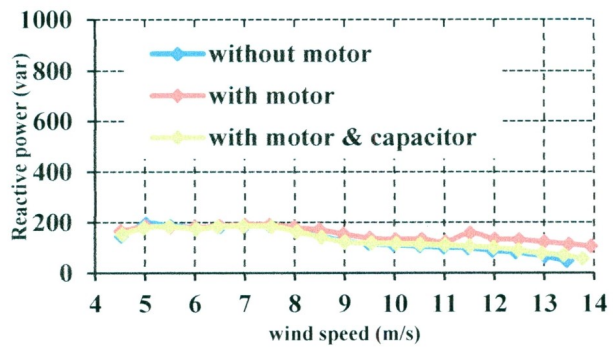
From Figure 2.9(a), it can be observed that the power curve for all the three cases i.e. without motor, with motor, and with motor and capacitors are about same. There is no effect of the induction motor and capacitors. Next, Figure 2.9(b) and Figure 2.9(c) indicate that the power factor is almost similar and reactive power is still less than 200var for the three cases. So, the inductive load and compensation capacitors have no effect on the power performance of this grid-connected small wind turbine.



(a)



(b)



(c)

Figure 2.9: Power performance comparison of turbine A with inductive and capacitive load a) power curve and b) power factor, c) reactive power

2.4.2 Experiments with Turbine B

The specifications of turbine B are as follows:

Rated Power: 1.3 kW
 Rated wind speed: 12 m/s
 Power Regulation: Active – Inverter
 Maximum continuous output power: 1.4 kW
 Utility interconnection voltage and frequency trip limits and trip times:
 Programmable, Utility specific
 Total Harmonic Distortion (current): < 3%
 Trip limit and trip time accuracy: < 10%
 Grid Voltage: Single phase, 208V
 Voltage Tolerance: $\pm 5\%$
 Grid Frequency: 60Hz
 Frequency Tolerance: $\pm 0.00083\%$

2.4.2.1 Power performance without any Local Load

Figure 2.10 shows the turbine power curve generated from the data collected over a number of days. It indicates that wind turbine B has a nonlinear power curve and it is not consistent. Sometimes, the turbine goes into stall regulation too early, say at 8m/s or 10 m/s and remains stalled above that wind speed; which is due to the furling control system. At that time, it does not produce any power. The following three power curves are for the same operational conditions (i.e. without any local load, turbine is connected directly to the grid) but weather conditions were different as the data was collected for the different period. Three data sets are plotted in Figure 2.10.

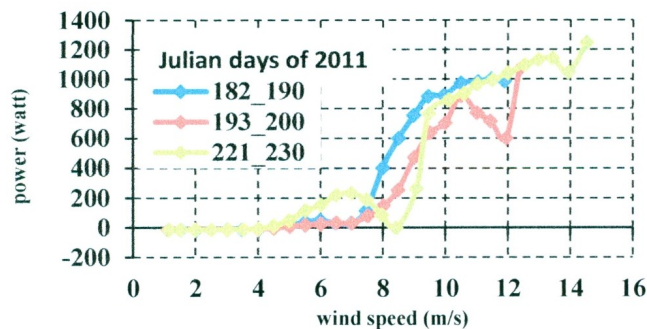
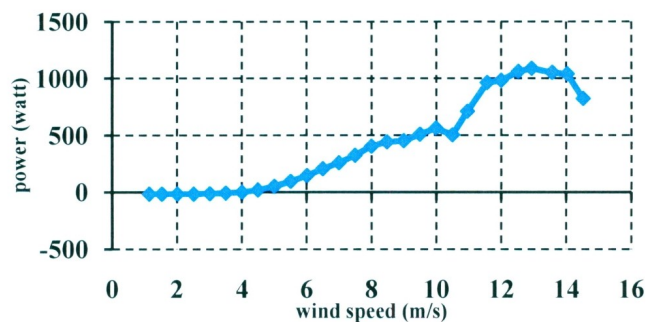


Figure 2.10: Power curve variation for turbine B under the similar conditions

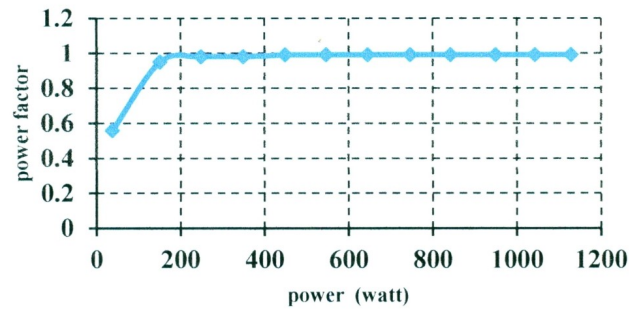
From Figure 2.10, it is clear that the power curve is inconsistent. For example, there was a sudden drop at 12m/s in the power curve during Julian days 193_200. Because of wind gust the wind turbine was stopped for a while but the average wind speed was 12m/s and the average power production was low. Therefore, it is very difficult to compare power curves with and without local load.

For our experimental comparison, one second data for fourteen days without any local load was collected and plotted following the same procedure as described above for wind turbine A. The active power and reactive power against wind speed were plotted in Figure 2.11. As the active power varies for the same wind speed, here we have plotted the power factor against the active power instead of power factor versus wind speed.

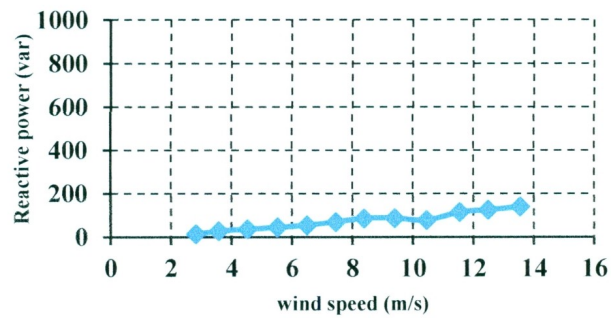
Figure 2.11(b) shows that the power factor is constant over a range of produced active power. When output power is more than 200W, the power factor becomes unity. From Figure 2.11 (c), there is insignificant change of reactive power with wind speed changes and reactive power is always less than 150 var.



(a)



(b)



(c)

Figure 2.11: Power performance of turbine B without any local load a) power curve, b) power factor and c) reactive power

2.4.2.2 Experiment with Heaters

Experiments were repeated similar to wind turbine A for resistive load. Turbine B was connected to phase A and phase B in the AC panel, so all the heaters were connected to phase A and/or Phase B, as shown in Figure 2.12 and data was collected and analyzed. Recorded data is plotted in Figure 2.13.

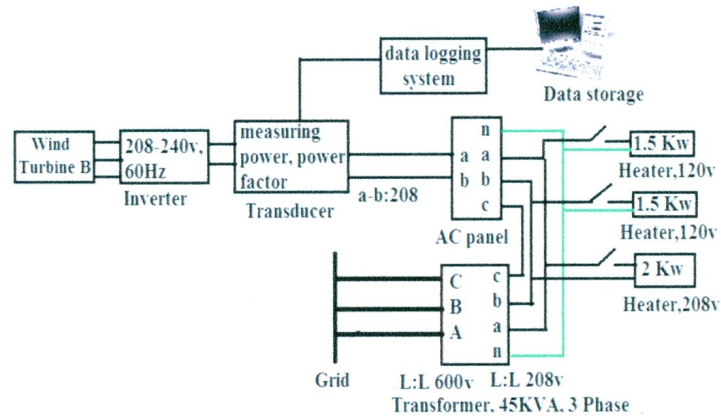
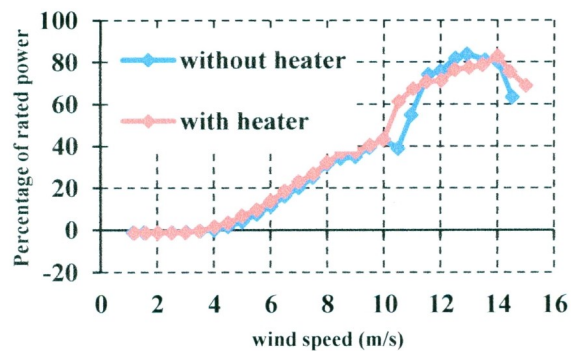
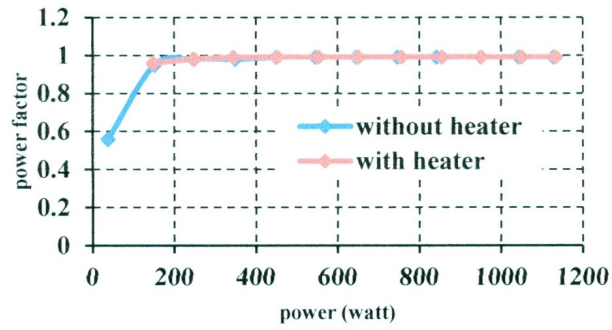


Figure 2.12: Block diagram for experiment setup with resistive load (heater) for turbine B

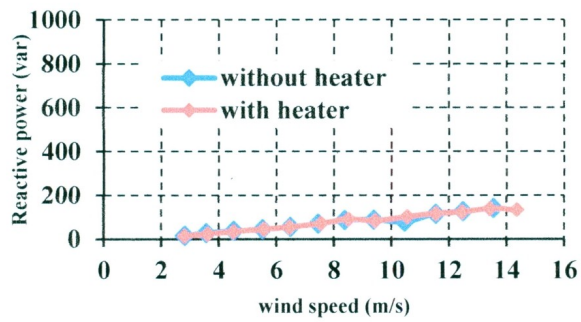
From Figure 2.13(a) we can see that there is a little change in the power curve. As mentioned earlier, the power curve is inconsistent for this wind turbine, so it is better to look at the power factor and reactive power. The power factor is also unchanged. From Figure 2.13(b), for both cases, the power factor was close to one when active power was greater than 200 watt. Figure 2.13(c) also shows that there is no significant change in reactive power. In both cases, reactive power increases gradually and it is always less than 150 var. Therefore, it could be concluded that there is no significant effect of resistive load on the power performance of turbine B.



(a)



(b)



(c)

Figure 2.13: Power performance comparison of turbine B with resistive load a) power curve, b) power factor and c) reactive power

2.4.2.3 Experiment with 5hp Induction Motor and Capacitors

The experiment was repeated for turbine B with inductive and capacitive load. Figure 2.14 below shows connection diagram for this set of experiments. As mentioned earlier, a Hioki meter was used before the transformer to measure the whole building power performance. Collected data was analyzed and it is plotted in Figures 2.15 & 2.16.

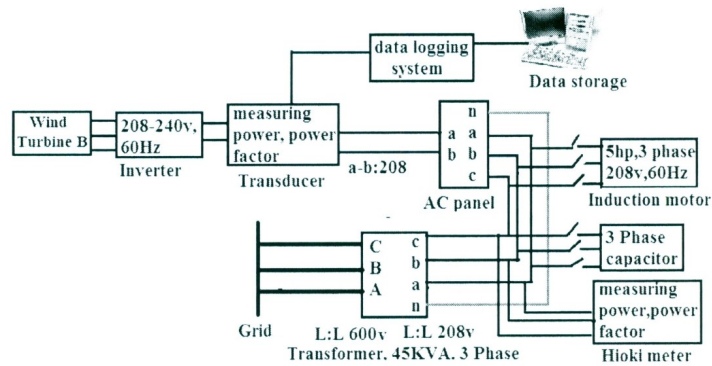


Figure 2.14: Block diagram for the experimental setup with an inductive load (motor) and capacitors for turbine B

In Figure 2.15, we can see that, when active power is greater than 200W power, in both directions (from grid or to grid), the power factor is very close to unity without the motor. When we connected the motor, power factor decreased, but when compensation capacitors were added($34.37\mu\text{F}$, 208v for each phase to phase) the power factor improved and increased to unity. It is noted that during the period when compensation capacitor was connected, maximum wind speed was around 9 m/s.

From Figure 2.16, when the system was without motor, reactive power was more or less 200 var. But when the motor was connected, the whole building demand for reactive power increased and it was greater than 1600 var. After that, capacitors were connected and the reactive power demand for the whole building was decreased.

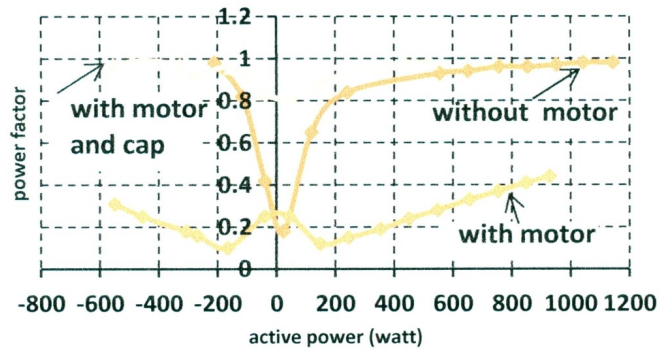


Figure 2.15: Power factor comparison of the whole building with inductive and capacitive load connected to turbine B

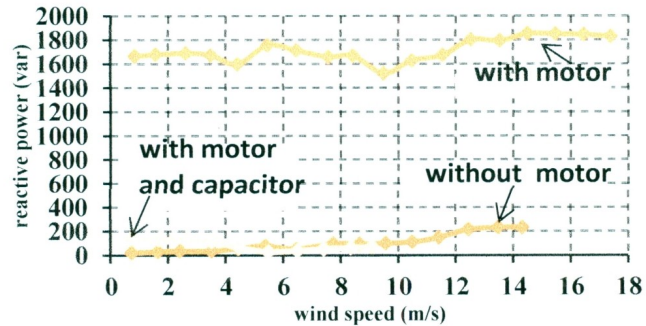
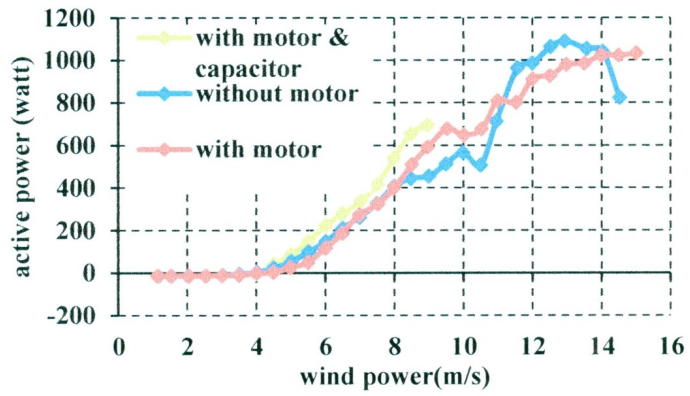
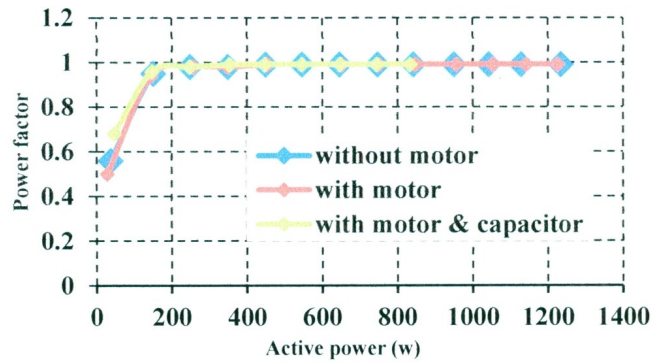


Figure 2.16: Reactive power comparison of the whole building with inductive and capacitive load connected to turbine B

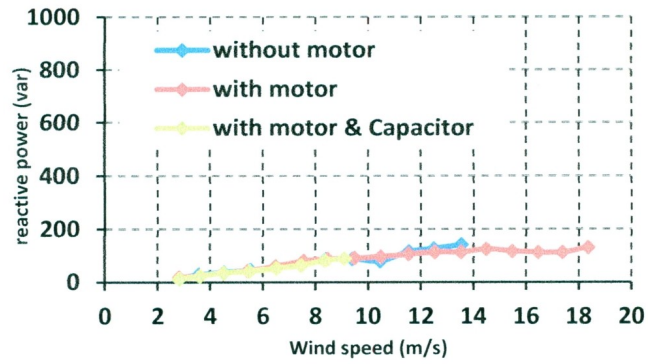
More test results are presented in Figure 2.17. Turbine transducer data was collected and analyzed as described previously for turbine A. From the plots in Figure 2.17(a), we can see that the power curve varied slightly. As this turbine power curve is inconsistent, it is better to compare the power factor and reactive power. From Figure 2.17 (b) and Figure 2.17(c), it can be seen that there is no significant effect of the inductive load and compensation capacitors on the turbine power factor and reactive power.



(a)



(b)



(c)

Figure 2.17: Power performance comparison of turbine B with inductive and capacitive load a) power curve, b) power factor and c) reactive power

2.5 Conclusion

This chapter described the power performance of two small wind turbines under variable load conditions. The active power performance, the power factor condition and the reactive power performance under resistive load, inductive load and compensation capacitors load have been presented in this chapter. From the data, it is concluded that there is no significant effect of load type on the power performance of a small grid-connected turbine. When experiments were done with a 5hp inductive motor, which consumes about 1600var, it was found that the turbine also had no effect on its reactive power production; thus, the power factor remained unchanged. The motor consumed the reactive power from the grid. Therefore, these experimental results show that the small wind turbine cannot produce any reactive power for inductive or capacitive load. The wind turbine inverter basically acts as a current source and its current phase angle is very close to the grid voltage phase angle.

Most of the small wind turbines are situated in remote locations isolated from the national power plant. If someone buys a small wind turbine to run a small motor for his/her business and connects the turbine to the grid, then the system will still consume reactive power from the grid and there could be loss or utility penalty for the reactive power. A control system should be developed so the owner can adjust the reactive power and power factor for an optimal operation and minimal reactive power from the grid. A proposed control system is discussed in the 4th chapter.

Chapter 3

DATA LOGGING AND POWER OPTIMIZATION OF A NOVEL VERTICAL AXIS WIND TURBINE

3.1 Introduction

In this chapter, a grid connected small vertical axis wind turbine system is analyzed for power optimization. The vertical axis wind turbine (VAWT) has two sets of blades. One set is fixed and guides wind into the second set of rotating blades. The rotor blades are distributed symmetrically about the vertical axis and thus it is independent of wind direction. To capture maximum power from wind, the stator makes a channel for the flow of air on the underside of the rotor blades. This novel type of stator also provides a rigid structure to the turbine to withstand wind speeds exceeding 60m/s. This wind turbine never needs to brake due to excessive wind thereby allowing it to capture wind over a large range of wind speeds. The maximum power extraction and optimization from such a novel vertical axis wind turbine is the main objective of this study. This VAWT system's inverter is based on Power Signal Feedback (PSF) control methodology for optimum power operation. PSF control depends on a look up table (i.e. a Maximum Power Point Tracking (MPPT) table)[47][48]. Generally computer simulation or experimental tests are used to create the MPPT table and this is the difficult part of this methodology[49].

This chapter describes the MPPT table developed mathematically for the novel VAWT. Power production data of this wind turbine was logged for a period of time to determine

its power curve. A simulation model of the VAWT has also been developed to validate the MPPT table.

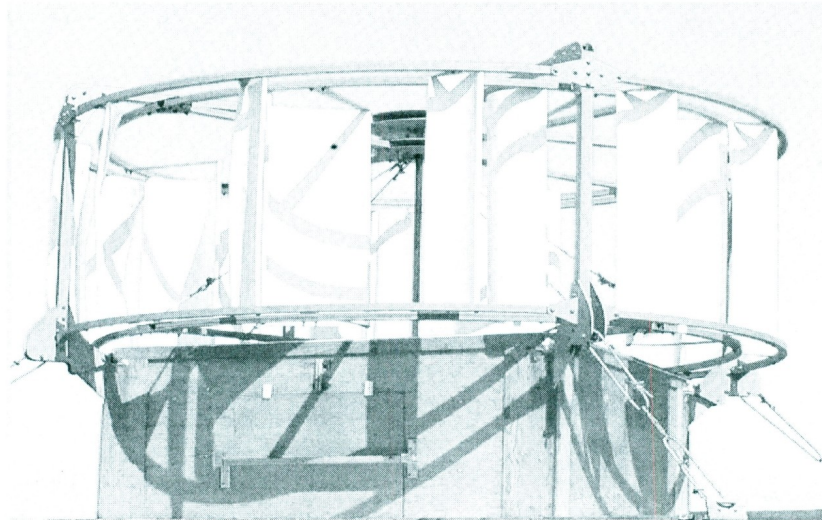


Figure 3.1: Vertical Axis Wind Turbine of this research

3.2 Technical information of the turbine and generator

The technical information of the wind turbine and the generator was collected from the corresponding manufacturers. This drag type VAWT rotates slowly with high torque and a gearbox is used to match the turbine and the generator. Gear box is discussed in section 3.5.

Wind Turbine Specifications:

Diameter / Height: 4m/1.5m
Cut-in wind speed : 2 m / s
Maximum wind speed: 60 m/s
Power at 15m/s: 1.3 kW
Power at 25 m/s: 4.4 kilowatts
Power at 40 m/s: 10 kW
Rotation speed: from 0 to 120 turns / min
Power control: Electronic Direct Torque Control

The turbine manufacturer also provided wind turbine test data for wind speed, optimum rotation and maximum power. Data is tabulated in Table 3.1

Table 3.1: Turbine optimum rotation and maximum power data from the manufacturer

Wind speed(m/s)	K_{opt} (rpm)	P_{max} (watt)
2	4.1268	11.45
4	8.2536	44.98
6	12.38	116.06
8	16.5072	257.75
10	19.9462	458.23
12	24.34812	773.27
14	27.512	1174.23
16	30.951	1575.19
18	34.39	2133.67
20	38.5168	2906.95
22	42.6436	3665.91
24	46.7704	4439.19
26	50.8972	5155.19
28	55.024	5914.15
30	59.1508	6644.47

Here,

K_{opt} =Optimum rotational speed of blades

P_{max} =Maximum power produced for optimum rotation of blades.

Generator Specification:

The generator of the system is a Permanent Magnet Generator (PMG). All the technical data of the generator are provided in Table 3.2.

Table 3.2: Generator information obtained from the generator manufacturer

Number of revolutions (RPM)	Current ¹ (A)	Voltage ¹ (V)	Power (watt)	Torque (N- m)
0	0	0	0	0
20	1.7	31.8	54	42.1
40	3.7	64.4	238	76.6
60	5.6	95.3	534	106.7
80	7.5	125.8	944	135.9
100	9.2	154.6	1422	162.6
120	11	183.6	2020	187.8
140	12.7	212	2692	211.9
160	14.3	238	3403	233.8
180	16	265	4240	255.5
200	17.5	296.1	5182	275.2
220	19	316.2	6008	294.2
240	20.5	340.5	6980	312.2

¹Voltage and current in the above table are rectified DC voltage and DC current.

3.3 Block diagram of the system

The vertical axis wind turbine is connected to PMG via a gearbox. The output of the generator is wild AC. It is rectified and the output DC is connected to an inverter. The inverter output is 208V and it is connected to the grid via a transducer and circuit breaker in the AC panel. The transducer is connected to a data logging system and the data logger is connected to a computer. The system block diagram is presented below in Figure 3.2

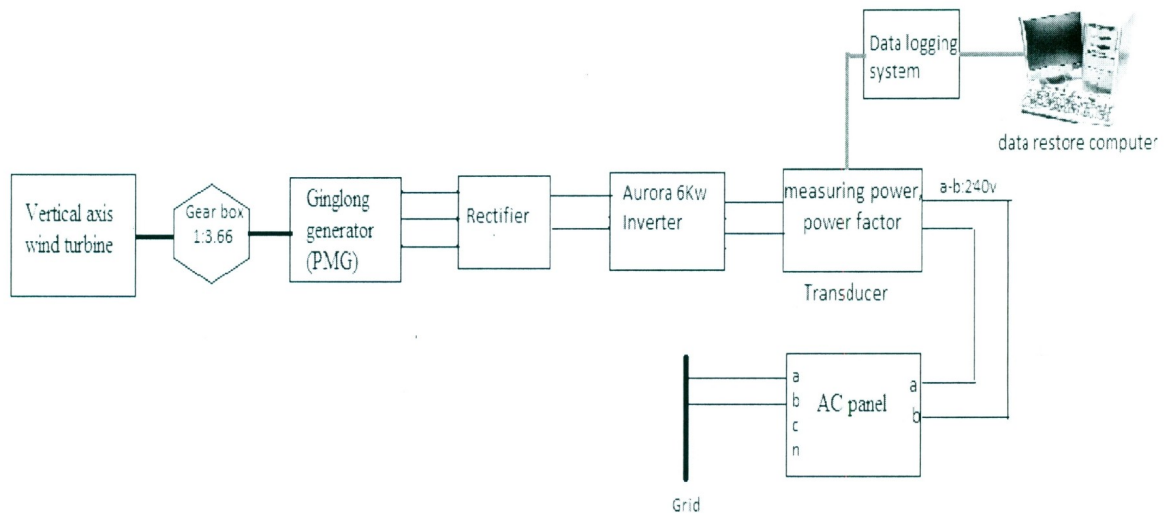


Figure 3.2: Block diagram of the wind turbine system

3.4 Power curve determination from the available turbine data

The wind turbine was installed and running for about two months before this research was started. Wind speed data and the output power data of the turbine were available for that period. Data was collected at a sampling rate of 1Hz. The available data was analyzed by using bins method and a power curve was derived. A Microsoft Excel based macro [50] has been created for analyzing the data. Detailed description of the macro is presented in Appendix A. The power curve is plotted and compared with manufacturer provided power curve in Figure 3.3.

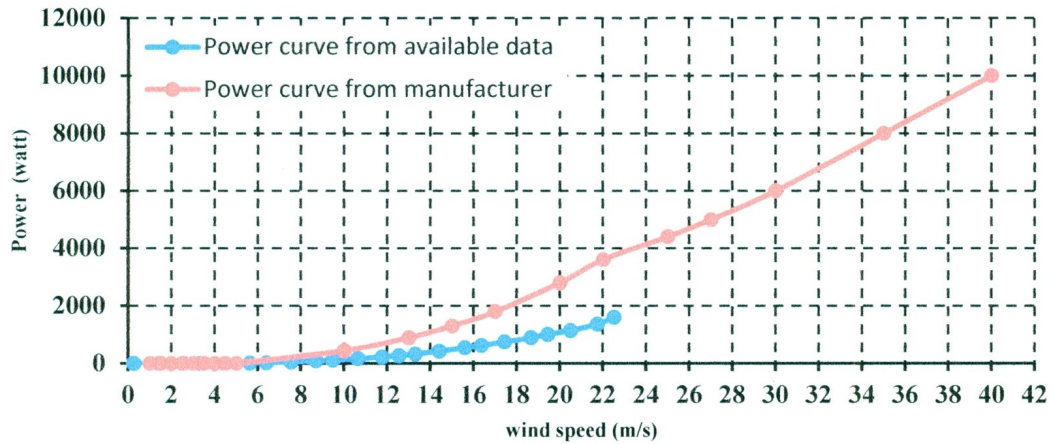


Figure 3.3: Initial power curve of the wind turbine and the manufacturer provided power curve

We also analyzed the power factor and we found that power factor is always more than .95 as expected.

From the above analysis we found that the wind turbine was not generating the power claimed by the manufacturer. The possible reasons are as follows:

- a. Improper scaling factor and offset value for the data logger
- b. Incorrect gearbox ratio
- c. Inaccurate MPPT table in the inverter

The scaling factors and offset value for the data logger were checked and found correct.

The gearbox ratio validation and the MPPT table derivation are described in details in the following sections.

3.5 Gearbox Ratio Analysis

Generally, in a wind energy conversion system (WECS), a gearbox is used to connect the low speed turbine to the high speed generator [49]. The current gearbox ratio is 1:3.66 and the manufacturer states its efficiency as 96%. As mentioned in chapter one, TSR is a ratio between the rotational speed of wind turbine blade and the wind speed. Maximum

power extraction occurs at an optimum TSR for a given wind speed. TSR is presented by equation 3.1 [51].

$$\lambda = \omega \frac{r}{V} \quad (3.1)$$

Here,

λ = Tip speed ratio,
 ω = blade rotational speed (rad/s),
 r = blade radius= 2m
 V = wind speed(m/s)

From the wind turbine data (Table 3.1), TSR of the turbine for various wind speed is calculated using equation (3.1) and presented in Table 3.3.

Table 3.3: Tip speed ratio calculation

V(m/s)	K_{opt} (rpm)	ω_{opt} (rad/sec)	λ_{opt}
2.00	4.13	0.43	0.43
4.00	8.25	0.86	0.43
6.00	12.38	1.30	0.43
8.00	16.51	1.73	0.43
10.00	19.95	2.09	0.42
12.00	24.35	2.55	0.42
14.00	27.51	2.88	0.41
16.00	30.95	3.24	0.40
18.00	34.39	3.60	0.40
20.00	38.52	4.03	0.40
22.00	42.64	4.46	0.41
24.00	46.77	4.90	0.41
26.00	50.90	5.33	0.41
28.00	55.02	5.76	0.41
30.00	59.15	6.19	0.41

From Table 3.3, it is found that the optimum tip speed ratio is almost constant and its average value is around 0.42.

From the manufacturer power curve in Figure 3.3, it is found that at 27 m/s wind speed, the turbine produces 5kW power.

From equation (3.2), $\lambda = \omega \frac{r}{V}$
 Or, $\omega = \lambda \frac{V}{r}$

At 27 m/s wind speed,

$\omega = (.42*27)/2$ Here, tip speed ratio, $\lambda=.42$
 $= 5.67 \text{ rad/s}$
 Or, $K = 54.17 \text{ rpm}$

So after the gearbox, the generator rotational speed should be $54.17*3.66=198.26 \text{ rpm}$.

From the Figure 3.4 we can see that at 198 rpm the generated power is almost 5kW.

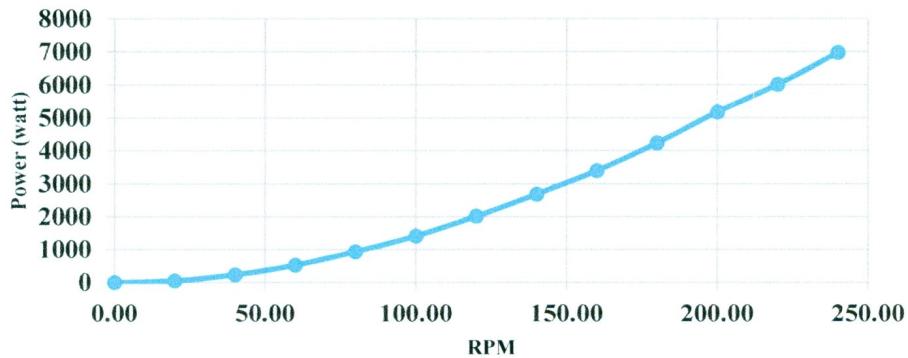


Figure 3.4 : Generator power vs. rpm

Again, from Figure 3.3, we can see that at 20 m/s wind speed, the turbine produces 2.8 kW. So at 20m/s, the turbine rotational speed is 40.12 rpm (calculated as previous case). After the gearbox, the generator rotational speed is $40.12*3.66=146.83 \text{ rpm}$. From the generator curve (Figure 3.4), at 146 rpm, power is approximately 2.8 kW. Therefore, it is proved that the gearbox ratio is correct for this VAWT system.

3.6 Determination of a Maximum Power Point Tracking (MPPT) Table

This section presents a detailed calculation of MPPT table for the VAWT. Calculation is based on all available information about the system. The system block diagram in Figure 3.5 indicates the values for MPPT table. The inverter PSF control system works on the basis of the DC voltage vs. power table and it is called MPPT table.

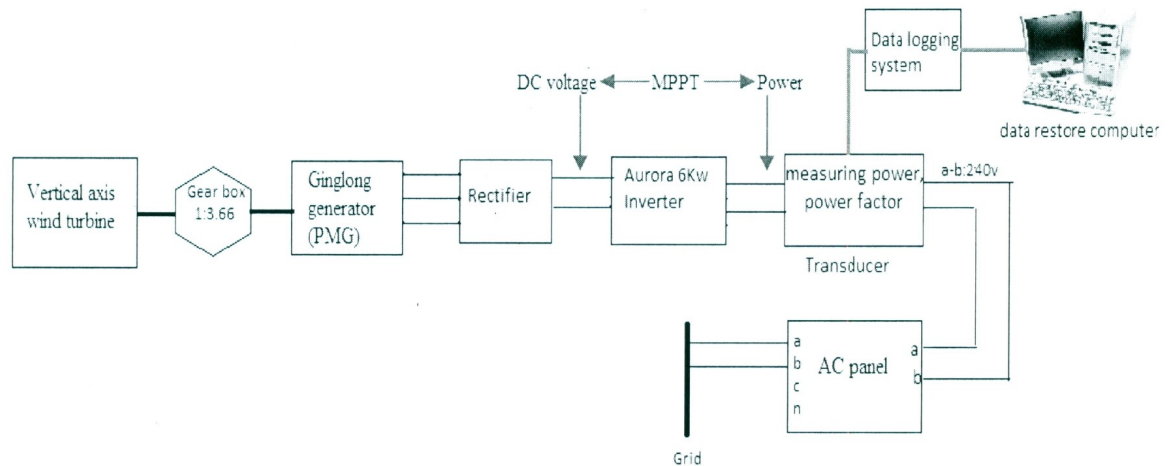


Figure 3.5: System block diagram indicating the use of MPPT table

3.6.1 Power calculation for the MPPT table

From the turbine data shown in Table 3.1, we can find the maximum power for a particular wind speed. This mechanical power is transferred to the generator via a gearbox and then converted to electrical power. The generator output power goes through the rectifier and the inverter before it is supplied to the grid at 240V. If we multiply this mechanical power with the gearbox efficiency (96%), alternator efficiency, rectifier efficiency and inverter efficiency, we can find out the inverter maximum power output.

3.6.2 Efficiency of the generator, rectifier and inverter

The generator and inverter efficiency vary with percentage of rated output power.

From the generator data shown in Table 3.2, we can determine the mechanical power by multiplying the torque and the rotational speed (rad/sec). Table 3.2 also provides the actual electrical output power data. From these two power data, we can calculate the generator efficiency (electrical power/mechanical power). The generator efficiency curve is shown below in Figure 3.6. As current and voltage data of the generator are rectified DC value (after the rectifier), the generator efficiency includes the rectifier efficiency.

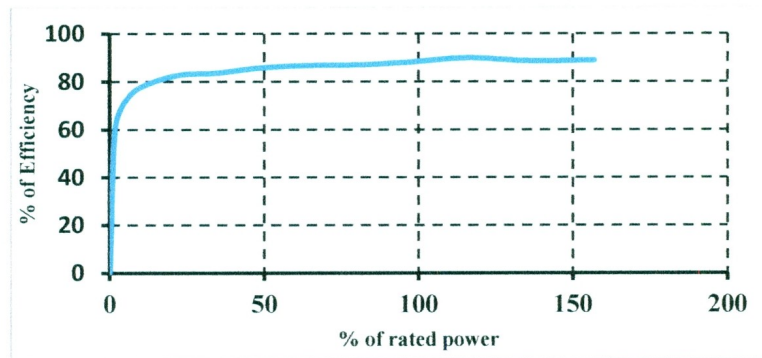


Figure 3.6: Generator efficiency including rectifier efficiency as a function of power.

The manufacturer has provided the inverter efficiency curve as shown in Figure 3.7.

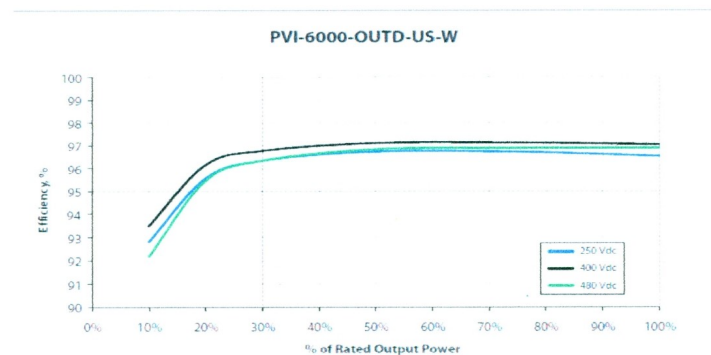


Figure 3.7: Inverter efficiency

The maximum power at the rotor is multiplied by gearbox efficiency. After that the power is converted to percentage of rated power of generator and then multiplied by the corresponding generator & rectifier efficiency. Again the power is converted to percentage of rated power of the inverter and multiplied by the corresponding inverter efficiency to determine the inverter output power and it is presented in Table 3.4.

Table 3.4: Calculated output power of the inverter

Wind speed (m/s)	Power_max_at rotor (watt)	Power_max_after gearbox (watt)	Power_max_after Generator & rectifier (watt)	Power_ma after inver (watt)
0.00	0.00	0.00	0.00	0.00
2.00	11.45	10.99	4.40	4.00
4.00	44.98	43.18	21.59	19.65
6.00	116.06	111.42	72.42	65.90
8.00	257.75	247.44	173.21	157.62
10.00	458.23	439.90	338.72	311.63
12.00	773.27	742.34	593.87	552.30
14.00	1174.23	1127.26	929.99	878.84
16.00	1575.19	1512.18	1255.11	1198.63
18.00	2133.67	2048.32	1741.07	1676.65
20.00	2906.95	2790.67	2372.07	2296.16
22.00	3665.91	3519.27	3054.73	2960.03
24.00	4439.19	4261.62	3750.23	3633.97
26.00	5155.19	4948.98	4355.10	4215.74
28.00	5914.15	5677.58	5109.83	4936.09
30.00	6644.47	6378.69	5677.04	5478.34

3.6.3 DC Voltage of the MPPT table

From the wind turbine data presented in Table 3.1, we can find out the optimum rotational speed for a particular wind speed i.e. the rotation per minute (rpm) of the blade at which the output power is maximum. If we multiply this rotation with the gearbox ratio (3.66), we will get the optimum generator rotor rpm.

Table 3.5: Optimum rotation of turbine and generator

Wind speed (m/s)	Turbine optimum rpm,	Gen. optimum rpm
0	0	0.00
2	4.12	15.08
4	8.25	30.20
6	12.38	45.31
8	16.5	60.39
10	19.94	72.98
12	24.34	89.08
14	27.51	100.69
16	30.95	113.28
18	34.39	125.87
20	38.51	140.95
22	42.64	156.06
24	46.77	171.18
26	50.89	186.26
28	55.02	201.37
30	59.15	216.49

From the generator data Table 3.2, we have generator rpm vs. voltage information. This voltage is the rectified DC voltage. From the available data, DC voltage vs. generator rpm graph is plotted in Figure 3.8.

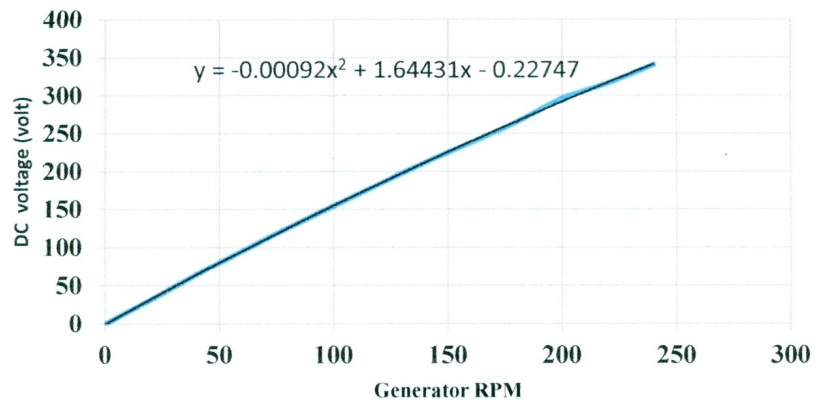


Figure 3.8: DC voltage vs. Generator rpm

Using curve fitting technique, the DC voltage and generator rpm are related by the polynomial equation of the curve as

$$y = -.00092x^2 + 1.64431x - .22747 \quad (3.2)$$

Here, y represents DC voltage and x represents generator rpm.

By using the equation 3.2, the voltage for each optimum generator rotational speed is calculated as shown in Table 3.6.

Table 3.6: Optimum rotational speed vs. DC Voltage

Wind speed (m/s)	Gen. optimum rpm	Gen. DC Voltage (V)
0	0.00	0.00
2	15.08	24.36
4	30.20	48.58
6	45.31	72.39
8	60.39	95.72
10	72.98	114.87
12	89.08	138.95
14	100.69	156.01
16	113.28	174.23
18	125.87	192.16
20	140.95	213.26
22	156.06	233.98
24	171.18	254.28
26	186.26	274.12
28	201.37	293.59
30	216.49	312.63

From Table 3.4 and Table 3.6, input DC voltage and output maximum power of the inverter are collected and presented in Table 3.7

Table 3.7: Input DC voltage and output power of the inverter

DC voltage(V)	Power (watt)
0.00	0.00
24.36	4.00
48.58	19.65
72.39	65.90
95.72	157.62
114.87	311.63
138.95	552.30
156.01	878.84
174.23	1198.63
192.16	1676.65
213.26	2296.16
233.98	2960.03
254.28	3633.97
274.12	4215.74
293.59	4936.09
312.63	5478.34

3.6.4 MPPT table

The minimum voltage of the inverter (V_{start}) is 55V. So MPPT table starts from 50V and the corresponding power is zero. As the inverter of this system has sixteen points for the MPPT table, two more points were created by extending the curve. The final MPPT table is presented in Table 3.8.

Table 3.8: MPPT table derived

DC voltage (V)	Power (watt)
50.00	0.00
72.39	65.90
95.72	157.62
114.87	311.63
138.95	552.30
156.01	878.84
174.23	1198.63
192.16	1676.65
213.26	2296.16
233.98	2960.03
254.28	3633.97
274.12	4215.74
293.64	4936.09
312.63	5478.34
330.00	6341.49
350.00	7261.25

When the MPPT table is programmed in the inverter, the inverter creates a MPPT curve from the table and it is shown below in Figure 3.9.

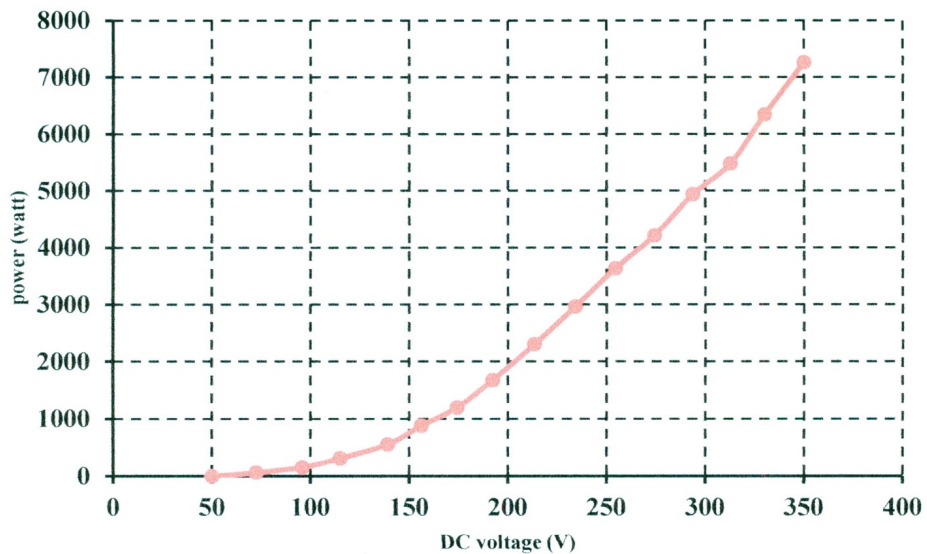


Figure 3.9: MPPT curve programmed in the inverter

When the VAWT runs with the MPPT table installed in the inverter, the inverter loads the generator according to the voltage from the curve shown in Figure 3.9. Say, if the generator produced DC voltage is 200V, the inverter will set the power to 2000 watt. So a particular torque will be applied to the turbine blade. If the turbine cannot provide that much torque to maintain the speed (speed at which the generator produces 200V), the rpm will decrease and the generator voltage will also decrease. The inverter will try with this new DC voltage and corresponding power. Now if the torque applied to the turbine blades is less than the previous torque, the rpm will be increased to maintain that torque and the generator DC voltage will also increase at this time. By this procedure, if the applied torque and the existing torque of the turbine blades match each other, the turbine will run at that speed and the output power will be maximized.

3.7 Dynamic Modeling and Simulation

A Matlab simulation model has been created for this VAWT system. Many articles are available regarding the simulation model of wind turbine e.g. [25][26][35][52][53]. The turbine manufacturer supplied data is used to create the turbine mathematical block. For permanent magnet generator, we have used built in block from Matlab simulation and changed the parameters to match with the particular generator used in this study. For rectifier and inverter, the universal bridge is used. A control system to extract maximum power from the turbine is also designed to implement the MPPT table.

Similar procedure was used to construct a simulation model for a 1.1 kW wind turbine system with active power control (extract maximum power) and reactive power control

and described in chapter four. Detailed description of that simulation model is presented in chapter four.

The developed simulation model is shown in Figure 3.10. After connecting all the blocks, we ran the simulation for different wind speeds and observed data for output power, DC voltage and TSR. We found that TSR is constant and it is around 0.42.

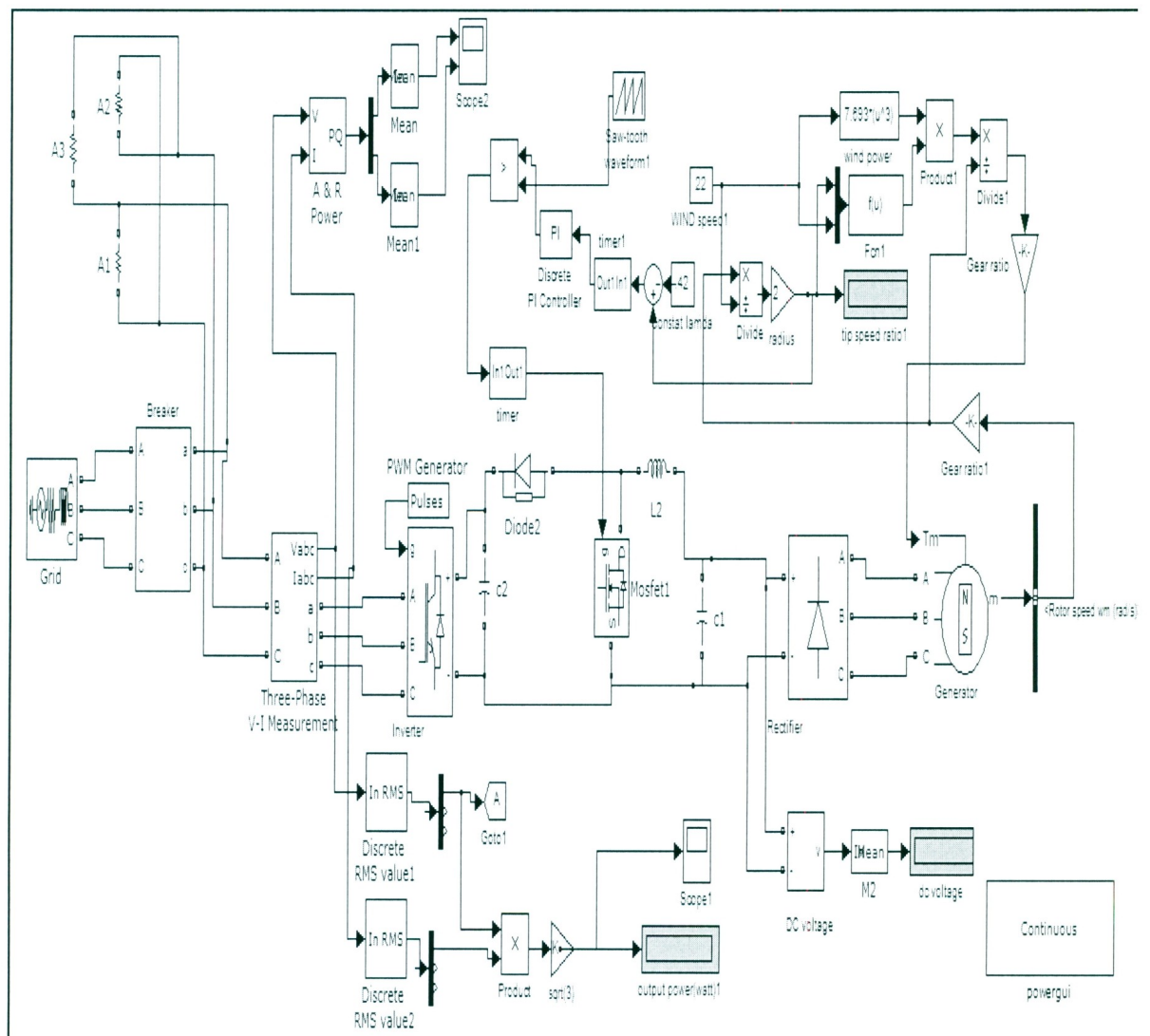


Figure 3.10: Simulation model of the VAWT

Simulated MPPT table and the calculated MPPT table are compared in Table 3.9.

Table 3.9: Calculated and Simulated Data Comparison

Wind speed (m/s)	Calculated from the data sheet			Simulation result data		
	DC Voltage (V)	Power (watt)	Tip speed ratio	DC Voltage (V)	Power (watt)	Tip speed ratio
2	24.36	4	0.43	15	4.1	0.26
4	48.58	19.65	0.43	39	31	0.35
6	72.39	65.9	0.43	66	88	0.39
8	95.72	157.62	0.43	92	173	0.40
10	114.87	311.63	0.42	118	288	0.42
12	138.95	552.3	0.42	144	442	0.42
14	156.01	878.84	0.41	168	640	0.43
16	174.23	1198.63	0.40	186	909	0.42
18	192.16	1676.65	0.40	204	1373	0.42
20	213.26	2296.16	0.40	224	1875	0.43
22	233.98	2960.03	0.41	241	2498	0.43
24	254.28	3633.97	0.41	258	3290	0.43
26	274.12	4215.74	0.41	275	4014	0.42
28	293.59	4936.09	0.41	311	4881	0.43

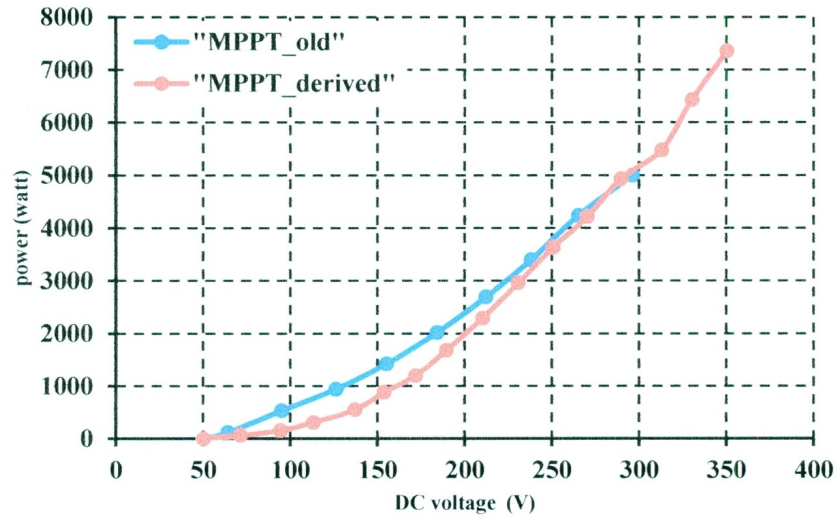
From the above table, it is found that the DC voltage of the derived MPPT table and the simulated model are almost equal but there are small discrepancies between the calculated and simulated powers. As few parameters of the generator are assumed to match the generator block with practical one, these small discrepancies are acceptable. Thus the derived MPPT table is verified in simulation before its field trials.

3.8 Data Analysis

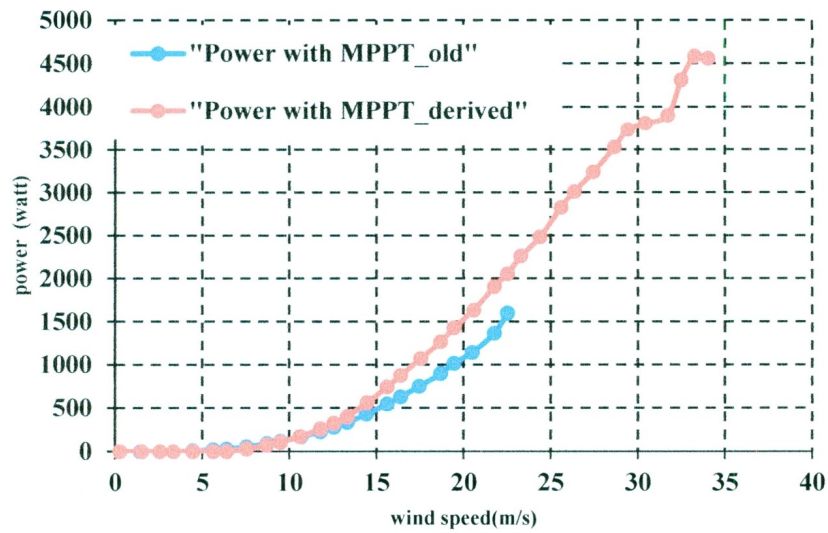
The derived MPPT table was installed in the inverter and the wind turbine was tested for few days. Data was logged for those days. From the collected data, power curve was

plotted and compared with the old power curve (Power curve shown in Figure 3.3).

Power curve and the MPPT table comparison are shown in Figure 3.11.



(a)



(b)

Figure 3.11: (a) MPPT_derived and old MPPT curves (b) Power performance with old MPPT and MPPT_derived

From the Figure 3.11 (b), it is found that the wind turbine produced more power with the derived MPPT table than with the old one (derived by the wind turbine installer). Thus it is clear that the derived MPPT is better than with the old one.

The derived MPPT table and the turbine simulation model are based on the system data from the manufacturers. To make sure that the derived MPPT table is optimal, two more MPPT tables were produced by shifting (up/down) the Y axis of the derived MPPT curve. These two MPPT tables are MPPT_test1 and MPPT_test2. The Y axis was shifted in such a way that it followed the same train of the original curve and located in the reasonable region.

MPPT_test1 and MPPT_test2 were installed in the inverter and data was logged for few days. In Figure 3.12, all the MPPT tables, and in Figure 3.13, their corresponding logged data based power curves are plotted and compared.

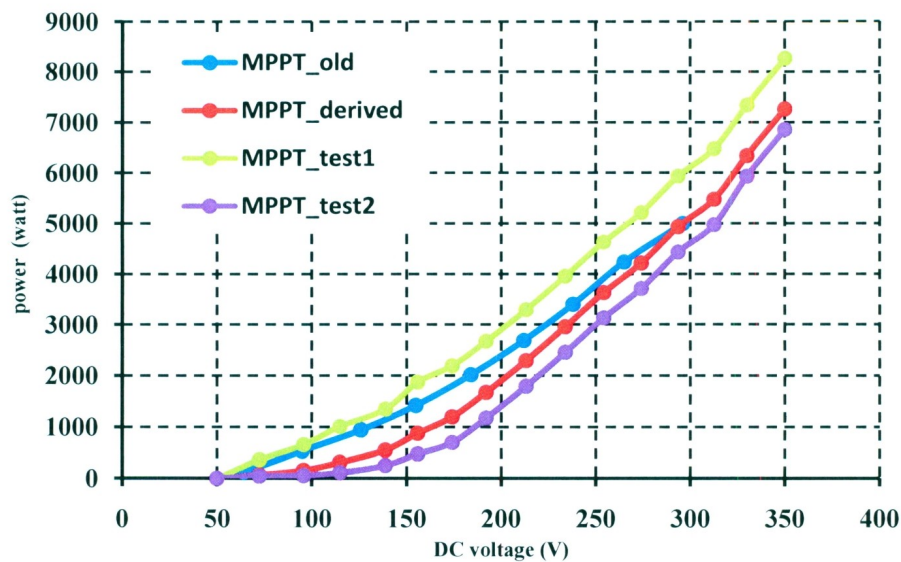


Figure 3.12: Four MPPT tables tested on the system

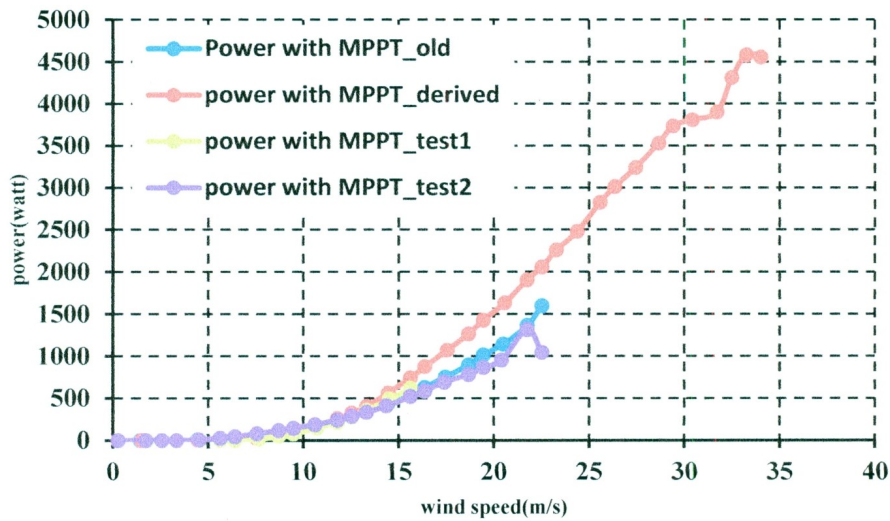


Figure 3.13: Out power comparison with different MPPT tables

From Figure 3.13, it is clear that the wind turbine produced maximum power with the derived MPPT. When wind speed is more than 15m/s, the wind turbine produced more power with the derived MPPT table than with the other MPPT tables. Therefore it can be said that the derived MPPT table is the best among all MPPT tables tested and it is correct and the best possible for the system.

3.9 Summary

In this chapter, initially the performance of a VAWT wind turbine was investigated using the already available data. Then step by step, the scaling factor and offset values for the data logger were checked and found that they are correct. The gearbox ratio was also verified. Then the MPPT table was mathematically derived. A simulation model of the system was built and the derived MPPT table was verified by using the model. Derived MPPT table was programmed into the system. Data was collected with the derived MPPT table. Two more variations of MPPT tables were also tested and data was collected. After

a detailed comparison, we can see that the system power performance with the derived MPPT is optimal. The derived MPPT curve is the best among all the power curves including MPPT curve suggested by the installer.

Chapter 4

Control System Design for Active and Reactive Power Control of a Small Grid Connected Wind Turbine

4.1 Introduction

Most of the commercially available small wind turbine-inverters are not designed to provide the required reactive power to its local load as described in chapter two. If a small wind turbine can provide some of the required reactive power, it will decrease the system reactive power demand from the grid. Thus it will decrease the losses in the distribution system and transformer power transfer capacity will be increased [37]. There are several technologies available to provide the reactive power, such as static var compensator (SVC) and static synchronous compensator (STATCOM) [43] [54], but all these technologies need extra equipment and extra costs.

The reactive power of a grid tie inverter depends on inverter output current which can be controlled by adjusting the modulation index and phase angle of the pulse width modulation generator [43]. In this chapter, a control system for control of reactive power along with maximum power point tracking (MPPT) operation has been developed for a small horizontal axis wind turbine. Detailed system modeling and simulation results are presented in the following sections.

4.2 Some Small Wind Turbines Issues

Most commercial small wind turbines are in the 1-10kW range. To investigate the power production characteristics under variable electrical loads, a bunch of experiments have been done and explained broadly in chapter two. From that chapter it is clear that most of the commercially available small wind turbines cannot produce reactive power when required. Figure 2.8 shows the reactive power drawn from the grid when an inductive motor is connected between the grid and turbine. Figure 2.16 shows the test result of reactive power drawn from the grid for another wind turbine. It is clear that when an inductive motor was connected, all the reactive power came from the grid, and the wind turbine inverter did not contribute to the reactive power. A local capacitor can help to compensate for that and ensure the required reactive power. But, a local capacitor can provide a fixed amount of reactive power not related to the load and such capacitors are costly. It would be ideal if a wind turbine inverter can also provide the reactive power for the local load. It could be achieved by a modification to the inverter control as proposed below.

4.3 Small Wind Turbine Configuration for this Research

In this research, a small horizontal axis wind turbine system similar to a practical one has been considered. The system consists of a 1.1 kW wind turbine, rectifier, DC-DC converter, inverter, transformer, grid, and the control system. A block diagram of the system is presented in Figure 4.1.

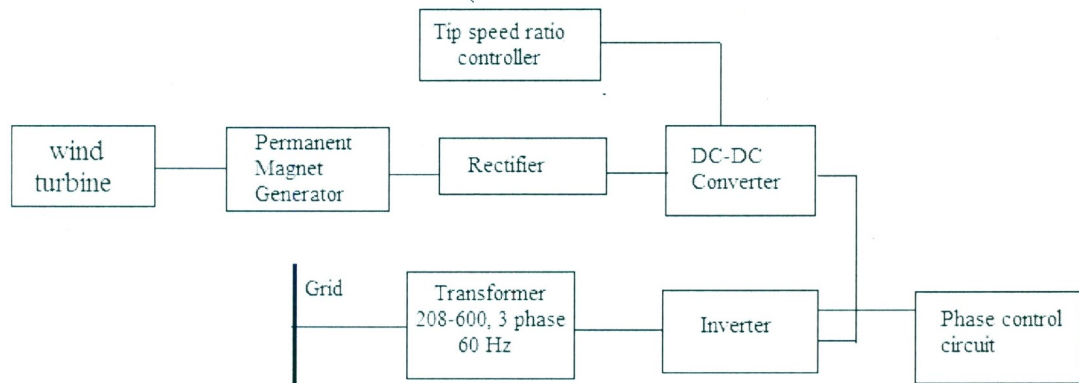


Figure 4.1: Block diagram of a small wind turbine system

4.4 System Modeling

The main parts of the system are the wind turbine, permanent magnet generator and the power electronics.

Wind turbine:

The wind turbine used in this study is a 1.1 kW system with a rated wind speed of 12 m/s.

The well-known equation of wind turbine power is:

$$P = .5\rho AV^3 C_p \quad (4.1)$$

$$C_p = f(\lambda) \quad (4.2)$$

$$\lambda = \omega \frac{r}{V} \quad (4.3)$$

Here:

P = Power (watt)

ρ = air density (Kg/m³)

A = rotor blade area (m²)

V = wind speed (m/s)

C_p = Power Coefficient,

λ = Tip speed ratio,

ω = rotor blade rotation (rad/s)

r= blade radius=0.9m

For this particular wind turbine, a maximum value of C_p is assumed as 0.5 and it occurs when the tip speed ratio is 6. Generally C_p increases with tip speed ratio increases for variable speed wind turbine until C_p reaches its maximum value and after that it decreases with tip speed ratio increases [55] [56] [57]. The following equation (4.4) represents a typical C_p - λ characteristic where C_p is maximum (0.5) when λ is equal to 6. This equation is used to define the C_p - λ relation of this particular small wind turbine.

$$C_p = -0.014\lambda^2 + 0.169\lambda - 0.002 \quad (4.4)$$

The wind turbine is simulated in Matlab Simulink using equations (4.1), (4.2) and (4.3) and it is presented in Figure 4.2.

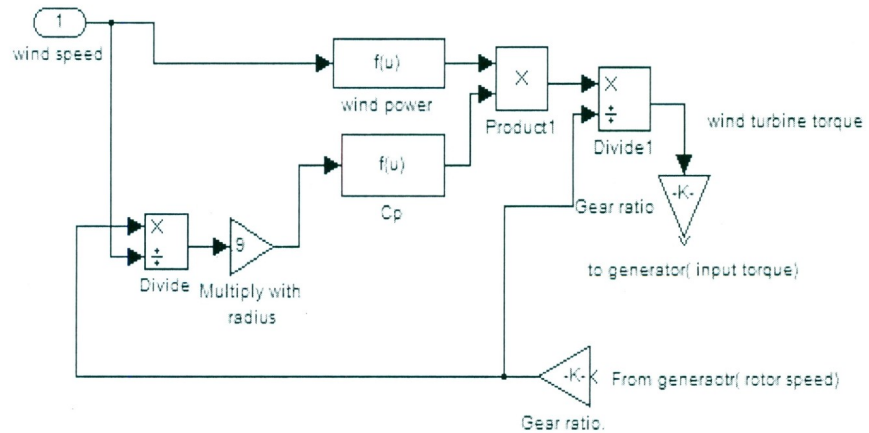


Figure 4.2: Wind turbine model

Permanent Magnet Generator:

For this system, a permanent magnet synchronous generator is used. The generator is 1.4 kW, 4 pole machine. The generator is modeled using the following equations [58] [59]:

$$\frac{d}{dt} i_d = \frac{v_d}{L_d} - \frac{R}{L_d} i_d + \frac{L_q}{L_d} p \omega_r i_q \quad (4.5)$$

$$\frac{d}{dt} i_q = \frac{v_q}{L_q} - \frac{R}{L_q} i_q + \frac{L_d}{L_q} p \omega_r i_d - \frac{\lambda_a p \omega_r}{L_q} \quad (4.6)$$

$$T_e = 1.5p[\lambda_a i_q + (L_d - L_q) i_d i_q] \quad (4.7)$$

Where,

L_q, L_d = q and d axis inductances
 R = Resistance of the stator windings
 i_q, i_d = q and d axis current
 V_q, V_d = q and d axis voltage
 ω_r = angular velocity of the rotor
 λ_a = Amplitude of the flux
 p = pole pairs number
 T_e = Electromagnetic torque

Power Electronics:

The generator is connected to a rectifier as shown in Figure 4.1. A simple diode bridge rectifier has been used in the model. The system output is two-phase. The rectifier is connected to an inverter via a DC-DC boost converter. The inverter is connected to a transformer. The transformer nominal power is 1.5kVA (208V to 600V, 3 phase).

A PI controller is used for the DC-DC boost converter switch control and a proportional controller is used for the phase control of the PWM inverter. Blocks from Simulink power system block-set are used to model the power electronics. Block parameters were adjusted accordingly. Block parameters are provided in the Appendix B. A full system model in Simulink is presented in Figure 4.3. The proposed control system is described below.

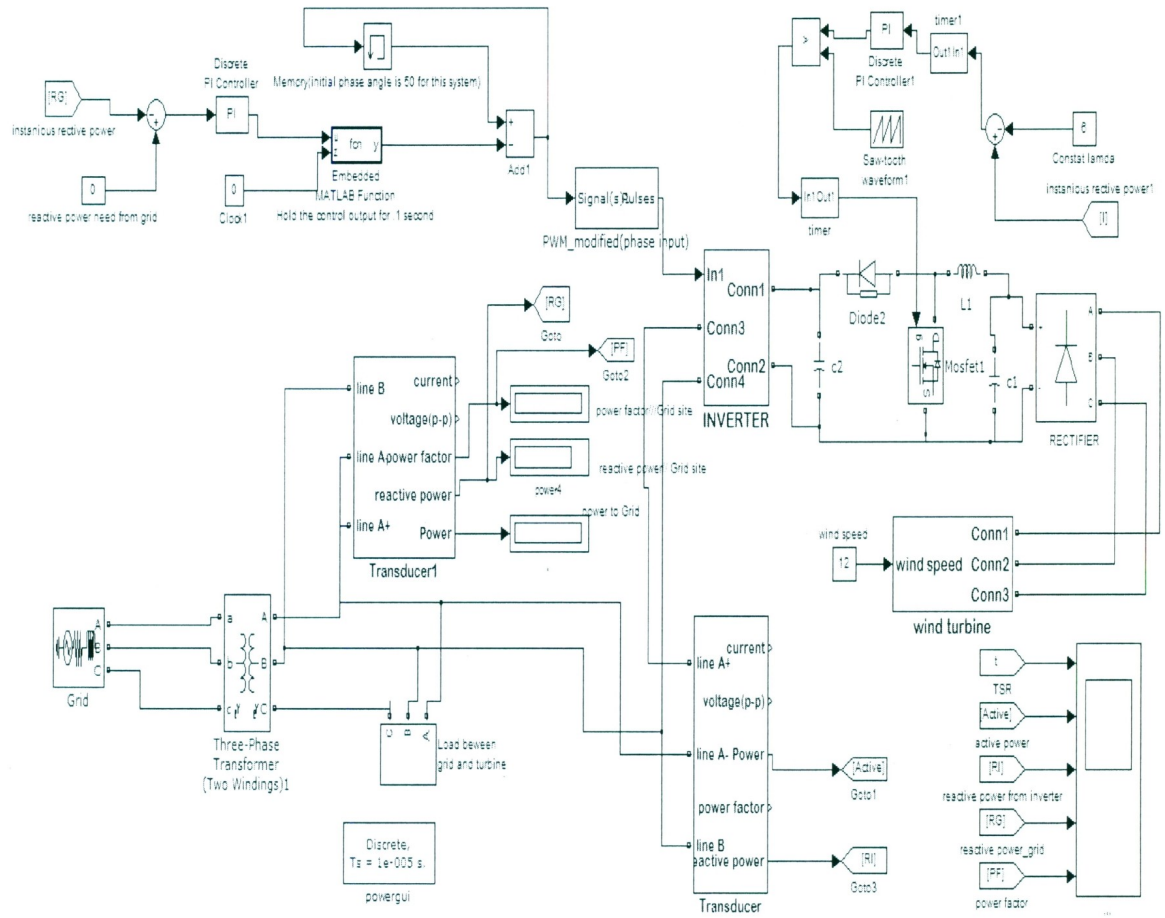


Figure 4.3: System modeling in Simulink

4.5 Control System Design

In this system, there are two different control units and they are independent. Detail description of these control systems is presented in the following sections.

4.5.1 Active Power Control System

To extract maximum power, the wind turbine has to rotate at a specific speed at a particular wind speed. When it passes through the air, the turbine blade creates turbulence and wake. If the subsequent blade arrives before the turbulence has vanished, it is not possible to extract maximum power from the wind but if the blade arrives just after the

wake has vanished, it can extract more power. For any turbine, this effect can be assigned a constant number referred to as optimum Tip Speed Ratio (TSR) [60]

The power coefficient of a wind turbine is maximized when it rotates at the optimum tip speed ratio. The main objective of this active power control system is to maintain the tip speed ratio at its optimum value for any wind speed. In this research, a PI controller is used with the DC-DC boost converter. A speed sensor measures the rotation speed of the turbine and an anemometer measures wind speed, and the instantaneous tip speed ratio is calculated with these two values. The instantaneous TSR is compared with the optimum TSR, and thus the error is calculated. (see Figure 4.3) The PI is used to correct the error in TSR. The output signal of the PI controller is compared with a triangular wave and a gate signal is generated for the DC-DC boost converter switch and thus the DC current from the generator to load is controlled. As the generator rpm depends on its load, indirectly the generator rpm can be controlled to a desired value. Again, the generator and the turbine are mechanically coupled; therefore the turbine is controlled to run at its optimum TSR. Figure 4.4 is a flow chart of the controller. If instantaneous TSR is the same as the desired TSR, then the PWM duty ratio is not changed. If instantaneous TSR is more than the optimum TSR, then the PWM duty ratio is increased or otherwise decreased. The control code also keeps the duty ratio within a set limit [61]. Therefore, the system active power is controlled by adjusting the DC input to the inverter. The designed controller also makes sure that the maximum power is extracted from the wind.

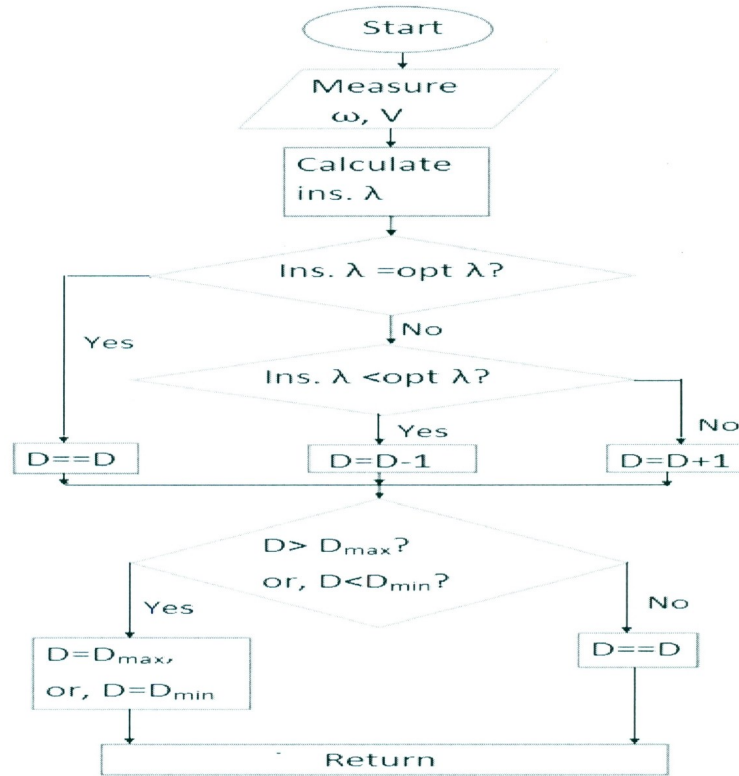


Figure 4.4: Flow chart for active power control

4.5.2 Reactive Power Control System

The PMG output for this system is a variable AC power that varies with the wind speed. The generator output is converted to DC power with a rectifier. The DC power goes through a DC-DC boost converter and is then converted to 60Hz, 208V, AC power with an inverter. In this research, a four pulse two leg inverter is used. The inverter pulse width modulation (PWM) generator is carrier- based. It creates pulses by comparing a triangular carrier waveform with a reference modulated signal as shown in the Figure 4.5. In this research, the triangle carrier signal is compared with the sinusoidal modulating signal. As the inverter has two legs therefore four pulses are needed for four switches.

The phase, frequency, and amplitude of the output voltage depend on the characteristics of the reference modulated signal. So by changing the modulating signal phase, the output voltage phase can be controlled [43].

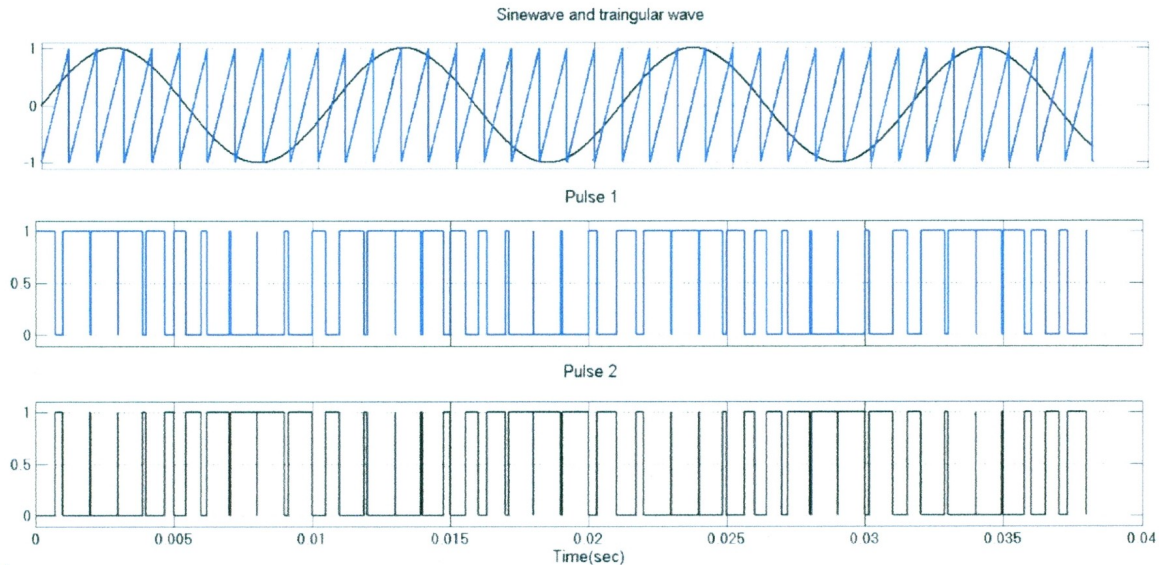


Figure 4.5: Reference signal, carrier signal and gate pulse for PWM

Here a Proportional controller and a memory block are used to control the phase angle of the output voltage. Memory block was added to avoid loop error. The controller works on the basis of the reactive power error. Reactive power error is the difference between the reactive power needed by the local load and the reactive power produced by the inverter. The memory block remembers the phase angle value that has been used during the previous time step. The controller changes its output according to the error, and using the memory value it adjusts the phase angle of the PWM generator to make the error equal to zero. With this control system the reactive power production of the wind turbine can be controlled and thus the total reactive power exchanges with the grid can be also controlled.

Controller parameters used in the simulation are adjusted by trial and error method and given below:

Active PI controller: $K_p = .5, K_i = .2$
 Reactive Proportional Controller: $K_p = .0045$

4.6 System Simulation and Results

After system modeling in Simulink, the total system has been simulated for different wind speeds and load demands. Here the simulation has been divided into three parts, which are demonstrated below.

4.6.1 Case study one

Condition:

Wind speed=12.5m/s,
 Load=purely resistive load,
 Simulation run time = One second

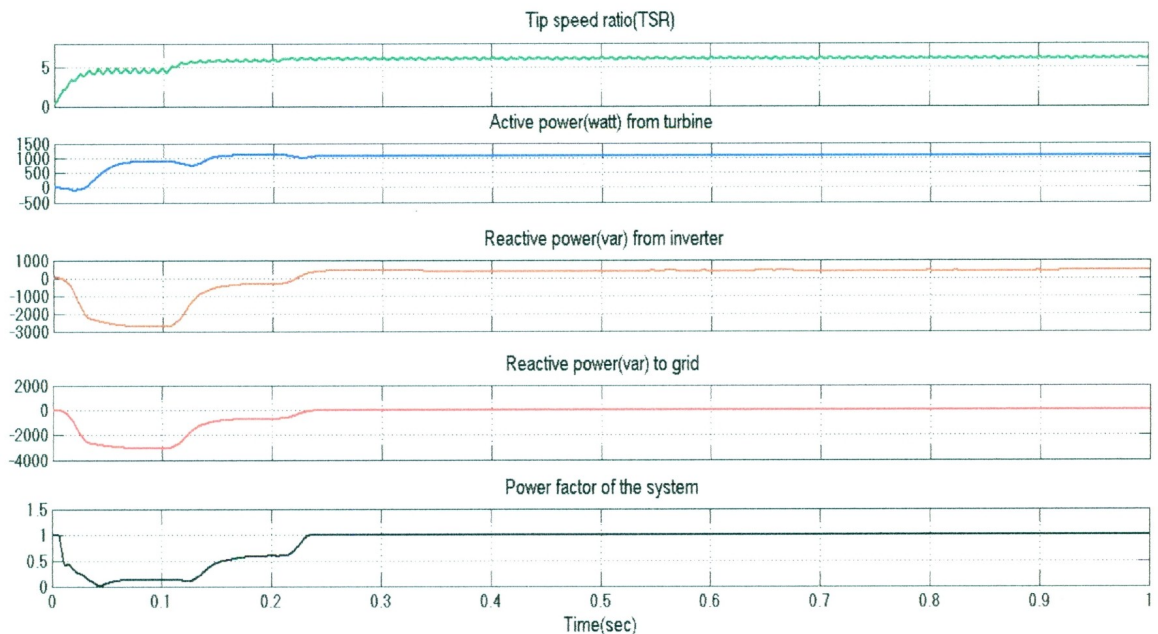


Figure 4.6: Case study one

In Figure 4.6 it is shown that TSR is constant and its value is six. Though the load is purely resistive, the inverter produces small amount of reactive power, as there is a transformer in the system. But from the grid side transducer it is clear that the total reactive power from the grid is equal to zero and for this reason the power factor is also very close to unity.

4.6.2 Case study two

Condition:

Wind speed=10m/s,
 Load=resistive and reactive load,
 Simulation run time = one second

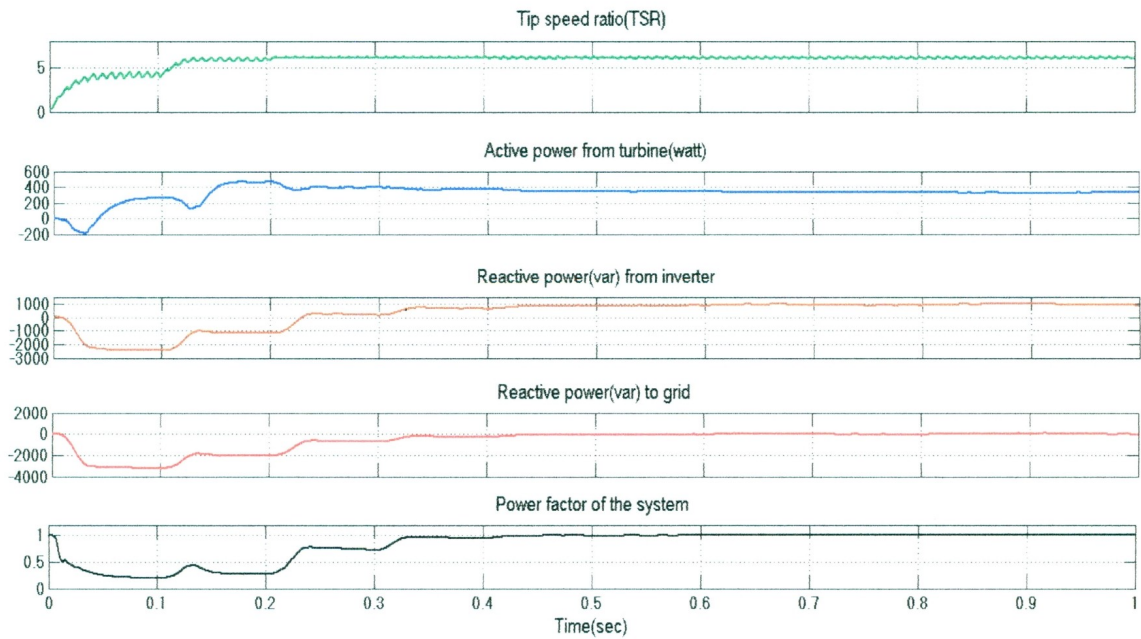


Figure 4.7: Case study two

In this case, as the load is not purely resistive, the inverter produces reactive power to meet the load demand and thus reduces the reactive power from the grid to zero. Thus the grid side power factor remains close to unity.

4.6.2 Case study three

Conditions:

Wind speed= variable,
 Load=resistive and reactive load,
 Simulation run time=3.5 second

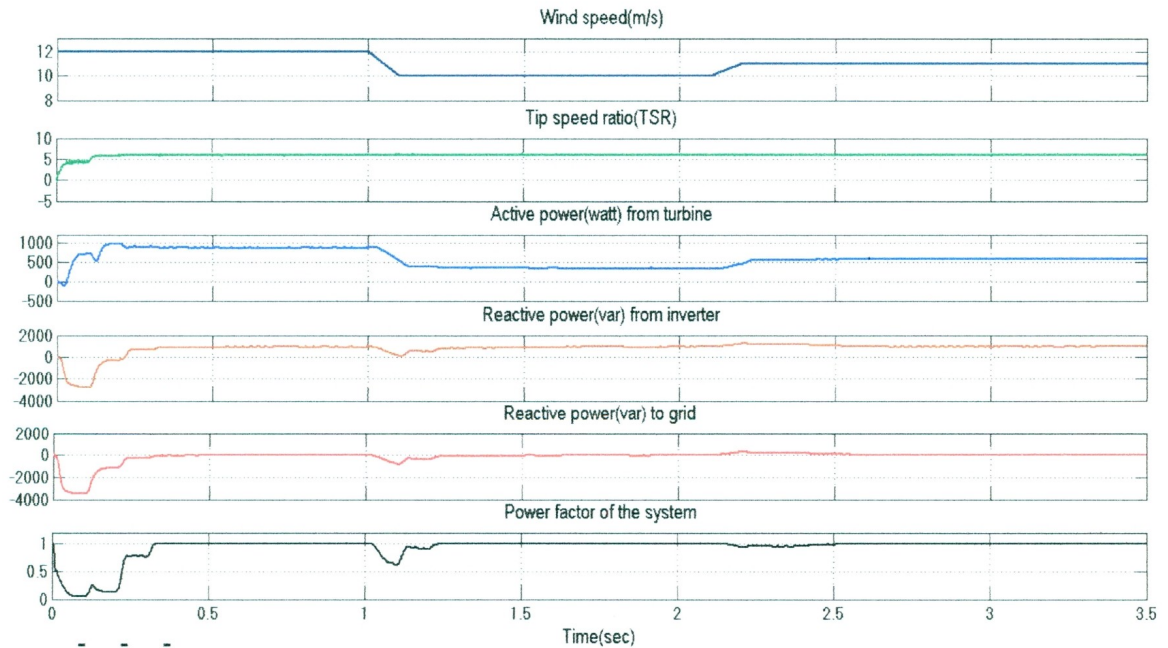


Figure 4.8: Case study three

In this case, there are sudden changes of wind speed and the stability of the system has been verified. When wind speed changes from 12m/s to 10m/s, the active power control circuit still maintains a TSR of six. Active power decreases as the wind speed decreases. But, as the load is not changed, the inverter produces the same amount of reactive power

as before. Thus the total reactive power exchange with the grid is still zero, and the system maintains a power factor close to unity. Again, at $t=2.1s$ when wind speed increases from 10m/s to 11m/s, active power increases but TSR, reactive power, and the power factor remain unchanged. This indicates that the designed control system extracts maximum power from the wind and provide reactive power for the local load. This model and the designed controllers could be simulated for any set of input conditions.

4.7 Summary

In this chapter, a control system has been developed for a small wind turbine system that extracts maximum power from the wind, and ensures that the system and local load consume zero reactive power from the grid. The wind turbine inverter is controlled so that it produces the required reactive power needed by the local load. The proposed reactive power control system is less complicated, as it does not require any rotational reference or use d-q machine theory. A wind turbine system with this type of technology will provide or consume zero reactive power to or from the grid. Some grid distributors have included an extra charge for wind turbine reactive power consumption. The proposed control system will avoid reactive power charge by not consuming reactive power from the grid.

Chapter 5

CONCLUSION AND RECOMMENDATIONS

5.1 Summary of the Research

The main objective of this research was to investigate the power performance of small wind turbines. For power performance analysis, we used two small wind turbines (turbine A and turbine B) from two different manufacturers. Turbine A is a 1.1 kW and turbine B is 1.3 kW rated small wind turbines. We connected different combinations of resistive, inductive and capacitive load between the turbine and the grid and collected data for those combinations. Those experiments took more than two months and it was done at WEICan, PEI. After the experiments, the data was analyzed following the IEC-61400-12-1 standard. From the experiments, we found results for two different turbines were similar. The conclusions of the experiments are:

- a. Commercially available small wind turbine power performance is not affected by the local loads.
- b. Small wind turbine inverters need to be configured to maintain power factor of the whole system close to unity.
- c. Small wind turbine inverters are unable to provide reactive power to load.

Another grid-connected small vertical axis wind turbine (VAWT) system was studied for optimum power operation in Nova Scotia. The VAWT's inverter has a Power Signal Feedback (PSF) based control unit to extract maximum power from wind and the control system needs a MPPT table. The VAWT system contains WT, gearbox, generator,

rectifier, and inverter. We analyzed the entire system and derived an optimum MPPT table. A Matlab simulink model of the VAWT system was also done along with a DC-DC boost converter and a PI controller. The main purpose of the control unit was to run the WT at such a speed that its TSR is optimum. The Simulink model was tested for different wind speed values and we collected the input DC voltage and output maximum power of the inverter and produced a MPPT table. The derived MPPT table was compared with the model based MPPT table and they were found similar. Thus the derived MPPT table was verified in simulation before field trials. After extensive field tests and data analysis of results we found that power performance of the turbine with the derived MPPT was optimized.

In the last stage of the research, a control system was also developed for active power and reactive power control of a small wind turbine system. In the proposed scheme, there are two independent control units but they work on the same system at the same time for two different objectives. The model was tested for three different conditions and found that the control system worked properly for different combinations of wind speed and load. With the proposed control system, a WT can extract maximum power form the wind and it can also control the reactive power production or maintain a zero reactive power from the grid.

The research contributions are as follows:

- a. Characterized the behavior of grid-connected small wind turbines under variable local loads and proposed improvements
- b. Developed a methodology to find an optimum MPPT table for small vertical axis wind turbine and field trials of MPPT table

- c. Designed and simulated a control system for active and reactive power control for a grid-connected small wind turbine.

5.2 Recommendations for Future Work

The MPPT table for the VAWT was derived by using the manufacturer provided data. In future, wind turbine system's experimental data (at least one year log) should be used to determine the MPPT table. We studied the wind turbine performance data for few days since there were only few windy days during the summer of 2012. When we divided the data into several bins according to wind speed range, there were not enough data points for some of the bins. Therefore, data collection for a long time is highly recommended. We were not able to do that since the NSERC funded project finished in five months.

To control the active power we used DC-DC boost converter and to control the reactive power we used the PWM generator. For future work a control system using only the PWM generator to control both the active and the reactive power is highly recommended. The grid that we used in the simulation is an AC-power source and it was connected only with one experimental wind turbine system. In future this type of control system should be modeled and simulated along with a wind turbine system which is connected to other wind turbines via the grid. In other words, full details of a real power system should be included in the model.

Bibliography

- [1] "World Energy Outlook," 2012.
- [2] Z. M. Salameh A. B. Cultura II, "Modeling and Simulation of a Wind Turbine Generator System," *Power and Energy Society General Meeting, IEEE, San Diego, CA*, 2011.
- [3] "BP Statistical Review of World Energy," June,2012.
- [4] Cheng Ke, Wang Zhongwei, He Yanchen, and Yang Guangjing, "The Comparison of Theoretical Potential Application," *Power and Energy Engineering Conference (APPEEC), Asia-Pacific*, 2012.
- [5] J.A. Orosa, E.J. Garcia-Bustelo, and A.C. Oliveira, "Low speed wind concentrator to improve wind farm," in *35th Annual Conference of IEEE, Industrial Electronics*, Porto, 2009, pp. 3605- 3608.
- [6] C.E.A. Silva, R.T. Bascope, and D.S. Oliveira, "Three-phase power factor correction rectifier applied to wind energy conversion systems," in *Twenty-Third Annual IEEE Applied Power Electronics Conference and Exposition*, Austin, TX, 2008, pp. 768 - 773.
- [7] R.D. Richardson and G.M. McNerney, "Wind Energy Systems," *Proceedings of the IEEE*, vol. 81, no. 3, pp. 378-389, March 1993.
- [8] J.A. Baroudi, V. Dinavahi, and A.M. Knight, "A review of power converter topologies for wind generators," in *2005 IEEE International Conference on Electric*

Machines and Drives, San Antonio, TX, 2005, pp. 458- 465.

- [9] M.M. Reis et al., "A variable speed wind energy conversion system connected to the grid for small wind generator," in *Twenty-Third Annual IEEE Applied Power Electronics Conference and Exposition*, Austin, TX, 2008, pp. 751-755.
- [10] C.E.A. Silva, D.S. Oliveira, L.H.S.C. Barreto, and R.P.T. Bascope, "A novel three-phase rectifier with high power factor for wind energy conversion systems," in *Power Electronics Conference, COBEP '09. Brazilian*, Bonito-Mato Grosso do Sul, 2009, pp. 985-992.
- [11] Seung-Ho Song, Shin-il Kang, and Nyeon-kun Hahm, "Implementation and control of grid connected AC-DC-AC power converter for variable speed wind energy conversion system," in *Applied Power Electronics Conference and Exposition, Eighteenth Annual IEEE*, vol. 1, Miami Beach, FL, USA, 2003, pp. 154-158.
- [12] Xiong Xin and Liang Hui, "Research on multiple boost converter based on MW-level wind energy conversion system," in *Electrical Machines and Systems, ICEMS 2005. Proceedings of the Eighth International Conference*, vol. 2, Nanjing, 2005, pp. 1046-1049.
- [13] Y. Higuchi, N. Yamamura, M. Ishida, and T. Hori, "An improvement of performance for small-scaled wind power generating system with permanent magnet type synchronous generator," in *26th Annual Conference of the IEEE, Industrial Electronics Society, IECON*, vol. 2, Nagoya, 2000, pp. 1037- 1043.
- [14] H.M. Suryawanshi, M.R. Ramteke, K.L. Thakre, and V.B. Borghate, "Unity-Power-

- Factor Operation of Three-Phase AC–DC Soft Switched Converter Based On Boost Active Clamp Topology in Modular Approach," *IEEE Transactions on Power Electronics*, vol. 23, no. 1, pp. 229- 236, Jan. 2008.
- [15] A.R. Prasad, P.D. Ziogas, and S. Manias, "An active power factor correction technique for three-phase diode rectifiers," in *20th Annual IEEE Power Electronics Specialists Conference*, vol. 1, Milwaukee, WI, 1989, pp. 58- 66.
- [16] V. Vongmanee and V. Monyakul, "Grid connected inverter with unity power factor for wind power applications," in *Industrial Electronics & Applications, ISIEA*, vol. 2, Kuala Lumpur, 2009, pp. 900- 903.
- [17] Z. Chen and E. Spooner, "Grid Power Quality with Variable-Speed Wind Turbines," *Power Engineering Review, IEEE*, vol. 21, no. 6, 2001.
- [18] M. Arifujjaman, M.T. Iqbal, J.E. Ouaique, and M.J. Khan, "Modeling and control of a small wind turbine," in *Canadian Conference on Electrical and Computer Engineering*, Saskatoon, Sask., 2005, pp. 778-781.
- [19] E., Forsyuth, T. Butterfield, C.P. Muljadi, "Soft–stall control versus furling control for small wind turbine power regulation," in *Windpower, Bakersfield, CA*, 1998.
- [20] J.T. Bialasiewicz, "Furling control for small wind turbine power regulation," in *IEEE International Symposium on Industrial Electronics*, vol. 2, Rio de Janeiro, Brasil, 2003, pp. 804- 809.
- [21] TomonbuSenjyu, Mohamed Orabi, Mohamed A.A. Wahab, Mohamed M. Hamada Mohamoud M. Hussein, "Simple Maximum Power Extraction Control for

- Permanent Magnet Synchronous Generator Based Wind Energy Conversion System," in *Japan-Egypt conference on " Electronics Communications and computers(JEC_ECC)*, Alexandria, 2012, pp. 194-199.
- [22] Abraham Lomi and Widodo Puji Mulayanto Aryuanto Soetedjo, "Modeling of Wind Energy System with MPPT Control," in *International conference on Electrical Engineering and informatics (ICEEI)*, Bandung, 2011., pp. 1- 6.
- [23] By Jogendra Singh Thongam and Mohand Ouhrouche, "MPPT Control Methods in Wind Energy Conversion Systems," in *Fundamental and Advanced Topics in Wind Power*, Rupp Carriveau, Ed.: InTech, 2011, ch. 15, pp. 339-360.
- [24] Athanasios Mesemanolis, Christos Mademlis, and Iordanis Kioskeridis, "A fuzzy-logic based control strategy for maximum efficiency of a Wind Energy Conversion System," in *International Symposium on Power Electronics, Electrical Drives, Automation and Motion (SPEEDAM)*, Sorrento, 2012, pp. 7-12.
- [25] Zoran Ivanovic, Milan Adzic, Vladimir Katic Evgenije Adzic, "Maximum Power Search in Wind Turbine Based on Fuzzy Logic Control," *Acta Polytechnica Hungaria*, vol. 6, no. 1, pp. 131-149, 2009.
- [26] Ali M. Eltamaly, "Modeling of Wind Turbine Driving Permanent Magnet Generator with Maximum Power Point Tracking System," *Journal of King Saud University, Engineering Science*, vol. 19, pp. 223-237, 2007.
- [27] Hui Li, P. McLaren, and K.L. Shi, "Neural network based sensorless maximum wind energy capture with compensated power coefficient," *IEEE Transactions on*

Industry Applications, vol. 41, no. 6, pp. 1548-1556, Nov.-Dec. 2005.

- [28] Chun-Yao Lee, Yi-Xing Shen, Jung-Cheng Cheng, Chih-Wen Chang, and Yi-Yin Li, "Optimization Method Based MPPT for Wind Power Generators," *World Academy of Science, Engineering & Technology*, vol. 60, p. 169, December 2009.
- [29] Jemaa Brahmi, Lotfi Krichen, and Abderrazak Ouali, "Sensorless control of PMSG in WECS using artificial neural network," in *6th International Multi-Conference on Systems, Signals and Devices*, Djerba, 2009, pp. 1-8.
- [30] G.D. Moor and H.J. Beukes, "Maximum power point trackers for wind turbines," in *IEEE 35th Annual Power Electronics Specialists Conference*, vol. 3, Aachen, 2004, pp. 2044-2049.
- [31] H. Gitano, S. Taib, and M. Khdeir, "Design and Testing of a Low Cost Peak-Power Tracking Controller for a Fixed Blade 1.2 kVA Wind Turbine," in *Compatibility in Power Electronics*, Gdansk, 2007, pp. 1-7.
- [32] E. Koutroulis and K. Kalaitzakis, "Design of a maximum power tracking system for wind-energy-conversion applications," *IEEE Transactions on Industrial Electronics*, vol. 53, no. 2, pp. 486-494, April 2006.
- [33] Joanne Hui and Alireza Bakhshai, "A Fast and Effective Control Algorithm for Maximum Power Point Tracking in Wind Energy Systems," in *World Wind Energy Conference*, Ontario, June 2008.
- [34] A.B. Raju, B.G. Fernandes, and K. Chatterjee, "A UPF power conditioner with maximum power point tracker for grid connected variable speed wind energy

- conversion system," in *First International Conference on Power Electronics Systems and Applications, IEEE*, Hong Kong, 2004., pp. 107-112.
- [35] A. Shaltout and M. A. L. Elshafei, N. Abdel-Rahim, H. Hagra, M. Zaher, M. Ibrahim M. Azouz, "Fuzzy Logic Control of Wind Energy Systems," in *Proceedings of the 14th International Middle East Power Systems Conference (MEPCON'10)*, Cairo University, Egypt, Cairo, 2010, pp. 935-940.
- [36] V. Galdi, A. Piccolo, and P. Siano, "Designing an Adaptive Fuzzy Controller for Maximum Wind Energy Extraction," *IEEE Transactions on Energy Conversion*, vol. 23, no. 2, pp. 559- 569 , June 2008.
- [37] Peiyuan Chen, P. Siano, B. Bak-Jensen, and Zhe Chen, "Stochastic Optimization of Wind Turbine Power Factor Using Stochastic Model of Wind Power," *IEEE Transactions on Sustainable Energy*, vol. 1, no. 1, pp. 19-29, April 2010.
- [38] A. Bouafia, F. Krim, and J.-P. Gaubert, "Fuzzy-Logic-Based Switching State Selection for Direct Power Control of Three-Phase PWM Rectifier," *IEEE Transactions on Industrial Electronics*, vol. 56, no. 6, pp. 1984-1992, June 2009.
- [39] P. Cortes, J. Rodriguez, P. Antoniewicz, and M. Kazmierkowski, "Direct Power Control of an AFE Using Predictive Control," *IEEE Transactions on Power Electronics*, vol. 23, no. 5, pp. 2516-2523 , Sept. 2008.
- [40] Jiabing Hu, Lei Shang, Yikang He, and Z.Z. Zhu, "Direct Active and Reactive Power Regulation of Grid-Connected DC/AC Converters Using Sliding Mode Control Approach," *IEEE Transactions on Power Electronics*, vol. 26, no. 1, pp.

210-222, Jan. 2011.

- [41] A. Cagnano, E. De Tuglie, M. Liserre, and R.A. Mastromauro, "Online Optimal Reactive Power Control Strategy of PV Inverters," *IEEE Transactions on Industrial Electronics*, vol. 58, no. 10, pp. 4549- 4558, Oct. 2011.
- [42] M. Saghaleini and B. Mirafzal, "Power control in three-phase grid-connected current-source boost inverter," in *IEEE Energy Conversion Congress and Exposition (ECCE)*, Phoenix, AZ, 2011, pp. 776-783.
- [43] M. Saghaleini and B. Mirafzal, "Reactive power control in three-phase grid-connected current source boost inverter," in *Applied Power Electronics Conference and Exposition (APEC), Twenty-Seventh Annual IEEE*, Orlando, FL, 2012, pp. 904-910.
- [44] P. Ladakakos, D. Foussis, E. Morfiadakis M.Koulouvri, "Measurement Systems Dedicated to wind turbine power quality applications," in *8th international conference on Harmonics and quality of power*, vol. 2, Athens, 1998, pp. 911-916.
- [45] International Electrotechnical Commission, CAN/CSA-C61400-12-1:07, Wind turbine-Part 12-1: Power performance measurements of electricity producing wind turbines. Ontario, Canada: CSA, October 2007.
- [46] S. J. Watson, D. Llombart and J. M. Fandos, A. Llombart, "Power Curve Characterization I: improving the bin method," in *International conference on renewable energies and power quality*, Zaragoza, 2005.
- [47] M. Ermis, H.B. Ertan, E. Akpınar, and F. Ulgut, "Autonomous wind energy

- conversion system with a simple controller for maximum-power transfer," *IEEE Proceedings B, Electric Power Applications*, vol. 139, no. 5, pp. 421-428, Sept. 1992.
- [48] R. Chedid, F. Mrad, and M. Basma, "Intelligent control of a class of wind energy conversion systems," *IEEE Transactions on Energy Conversion*, vol. 14, no. 4, pp. 1597-1604, Dec 1999.
- [49] Quincy Wang and Liuchen Chang, "An intelligent maximum power extraction algorithm for inverter-based variable speed wind turbine systems," *IEEE Transactions on Power Electronics*, vol. 19, no. 5, pp. 1242-1249, Sept. 2004.
- [50] Microsoft office- Excel. [Online]. <http://office.microsoft.com/en-ca/excel/>
- [51] Liqin Ni, D.J. Patterson, and J.L. Hudgins, "Maximum power extraction from a small wind turbine using 4-phase interleaved boost converter," in *IEEE Power Electronics and Machines in Wind Applications*, Lincoln, NE, 2009, pp. 1-5.
- [52] H.A. Yanto, Chun-Ta Lin, Jonq-Chin Hwang, and Sheam-Chyun Lin, "Modeling and control of household-size vertical axis wind turbine and electric power generation system," in *International Conference on Power Electronics and Drive Systems*, Taipei, 2009, pp. 1301-1307.
- [53] Yan Li, Fang Feng, Shengmao Li, and Yongjun Han, "Computer simulation on the performance of a combined-type vertical axis wind turbine," in *International Conference on Computer Design and Applications (ICCCA)*, vol. 4, Qinhuangdao, 2010, pp. 247- 250.

- [54] S.P. Gawande, N.A. Kubde, M.S. Joshi, and B.S. Sudame, "Reactive power compensation of wind energy distribution system using Distribution Static Compensator (DSTATCOM)," in *IEEE 5th India International Conference on Power Electronics (IICPE)*, Delhi, 2012, pp. 1-5.
- [55] Ming-Fa Tsai, Chung-Shi Tseng, and Yu-Hsiang Hung, "A novel MPPT control design for wind-turbine generation systems using neural network compensator," in *IECON 2012 - 38th Annual Conference on IEEE Industrial Electronics Society*, Montreal, QC, 2012, pp. 3521-3526.
- [56] G. Putrus, M. Narayana, M. Jovanovic, and Pak Sing Leung, "Maximum power point tracking for variable-speed fixed-pitch small wind turbines," in *20th International Conference and Exhibition Electricity Distribution - Part 1, 2009. CIRED 2009.*, Prague, Czech Republic, 2009, pp. 1- 4.
- [57] S. Bhowmik and R. Spee, "Wind speed estimation based variable speed wind power generation," in *Proceedings of the 24th Annual Conference of the IEEE ,Industrial Electronics Society*, Aachen, 1998, pp. 596-601 vol.2.
- [58] L.-A.Dessaint and YvaBonnassieux, Damien Grenier, "Experimental Nonlinear Torque Control of a Permanent-Magnet Synchronous Motor Using Saliency," *IEEE Transactions on Industrial Electronics*, vol. 44, no. 5, pp. 680-687 , Oct 1997.
- [59] MATLAB/SIMULINK and MATLAB/SimPower Systems are the products of The MathWorks, 3 Apple Hill Drive, Natick, MA 01760-2098, USA. [Online].
<http://www.mathworks.com>

- [60] J.D.M. De Kooning, B. Meersman, T.L. Vandoorn, and L. Vandeveldel, "Evaluation of the Maximum Power Point Tracking performance in small wind turbines," in *Power and Energy Society General Meeting, IEEE*, San Diego, CA, 2012, pp. 1-8.
- [61] A. J. Mahdi, W. H. Tang, and Q. H. Wu, "Estimation of tip speed ratio using an adaptive perturbation and observation method for wind turbine generator systems," in *IET Conference on Renewable Power Generation (RPG 2011)*, Edinburgh, 2011, pp. 1-6.

Appendix A

Data Analysis procedure using the developed Macro

Generally the data logger of a wind turbine collects the data and makes a file for one hour/one day and save that in a memory card. If we want to plot a power curve of a wind turbine for few days, we have to analyze all data set. To analysis the data automatically, two different types of software were used in this research. They are:

1. Macro sheduler
2. Microsoft excel based macro

Macro scheduler can record the activities that we do on a computer on daily basis. After recording, if we want to do the same tasks again, we have to play the record file and the software will do the analysis automatically. With this software we can make a record file for wind turbine data analysis that combine all raw data files in one single file.

Microsoft Excel based macro records all the tasks that we do in Excel. The wind turbine data are analyzed according to IEC 61400-12-1 standard as described in chapter two. By using equations (2.1) to (2.5) in Microsoft Excel, a macro has been created named “sugen.xlm”.

The procedure for using these two macros is described in the following section.

Initial steps:

1. A folder named “sugen5KW” is created in C drive.
2. “sugen.xlm” is copied in that folder.
3. Raw data files (.dat file) are also copied on that folder.
4. “macro_scheduler_setup.exe” is installed

It will also create a desktop shortcut. By clicking on that shortcut a window will open out as shown in Figure A-1.

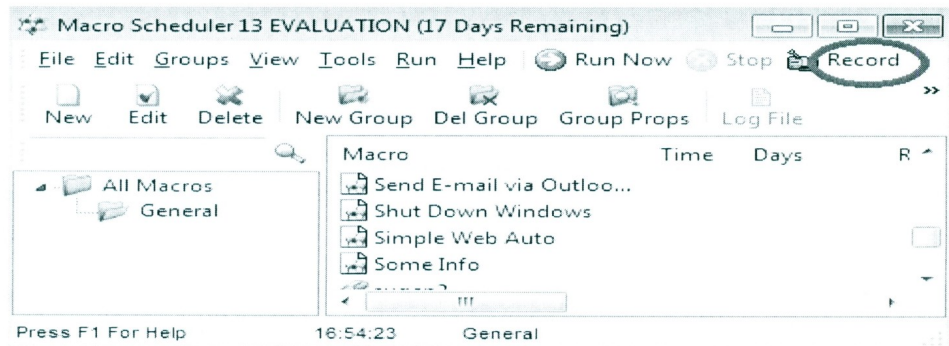


Figure A-1: Macro Scheduler record tab

Then the record tab is clicked and the window becomes as shown in Figure A-2.

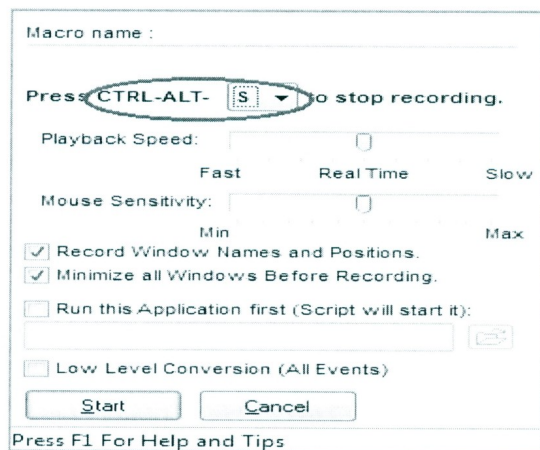


Figure A-2:Macro Scheduler file name

A name is given for the record macro. The key combination to stop the recoding is CTRL-ALT-S.

Macro recording procedure:

Start button on computer is clicked and “cmd” is typed as on Figure A-3.



Figure A-3: command file call

The below window will come up.

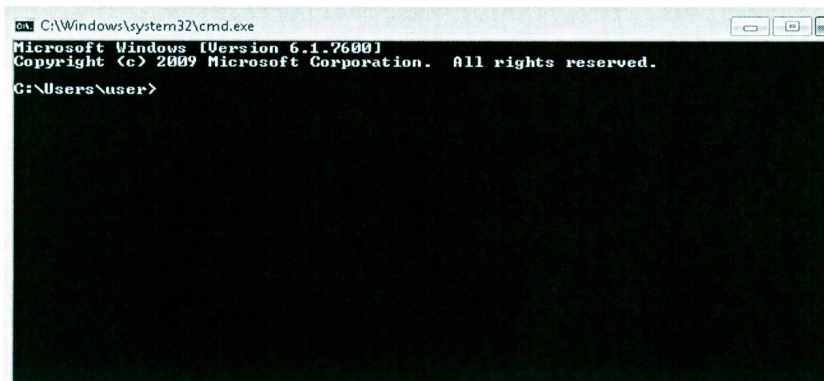
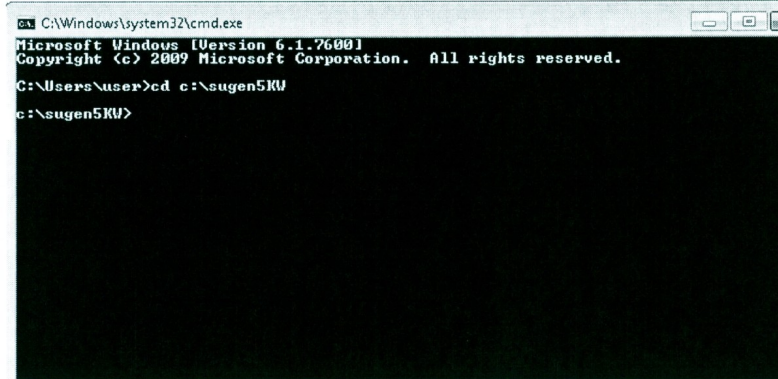


Figure A-4: Command file on PC (OS windows)

“cd c:\sugen5KW” is typed and enter key is pressed. The window will appear as shown in Figure A-5.



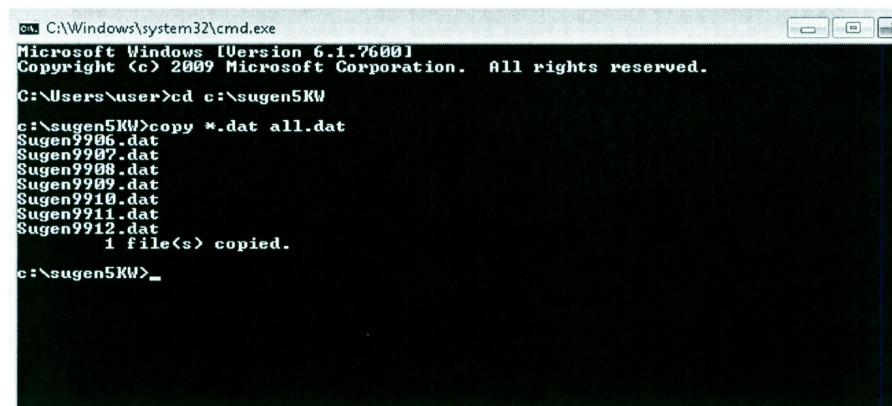
```
C:\Windows\system32\cmd.exe
Microsoft Windows [Version 6.1.7600]
Copyright (c) 2009 Microsoft Corporation. All rights reserved.

C:\Users\user>cd c:\sugen5KW
c:\sugen5KW>
```

Figure A-5: Folder select command window

After that, “copy *.dat all.dat” is typed and enter key is pressed again. (Note there is a space between the copy and *)

All the raw data files are combined in a single file and screen may appear as in Figure A-6.



```
C:\Windows\system32\cmd.exe
Microsoft Windows [Version 6.1.7600]
Copyright (c) 2009 Microsoft Corporation. All rights reserved.

C:\Users\user>cd c:\sugen5KW
c:\sugen5KW>copy *.dat all.dat
Sugen9906.dat
Sugen9907.dat
Sugen9908.dat
Sugen9909.dat
Sugen9910.dat
Sugen9911.dat
Sugen9912.dat
1 file(s) copied.
c:\sugen5KW>_
```

Figure A-6: Command to combined multiply files

Here we have to input some delay time because in future we may analyze a lot of data and at that time it will take few seconds more. For this purpose, the black window is closed after a 30 second delay.

Now for stopping the recording, CTRL-ALT-S is pressed.

The macro is saved in ‘document’ folder as .scp file. The file is copied in “sugen5KW” folder in C drive.

This macro we have just created varies from PC to PC. So we have to record this macro for each PC individually. After a macro is recorded for a PC, we don’t need to record for further analysis.

For each time before we analyze the data, we have to delete all the .dat from “sugen5KW” folder and follow the steps below.

- a. We have to copy all the new .dat files (those we want to analyze) and paste in that “sugen5KW” folder.
- b. Then .scp file is clicked. A window will open with a tab named continue. When we click continue we have to release the mouse immediately as the macro will use the cursor.
- c. After few moments we can see that a file named “all.dat” has been created in the “sugen5KW” folder.
- d. sugen.xlsm file on C:\sugen5KW is clicked

On sheet2, there will be a tab named Developer.

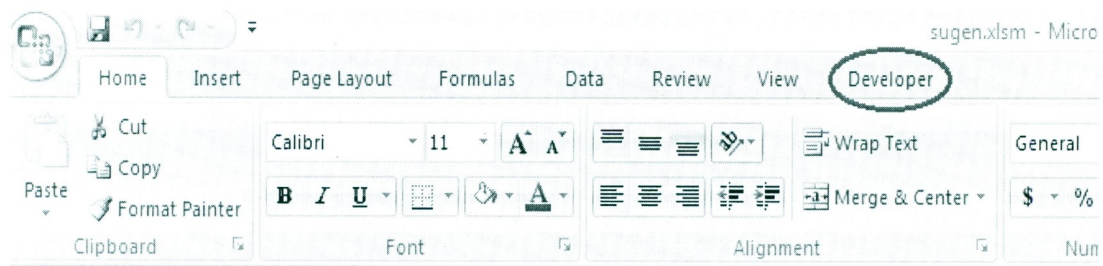


Figure A-7: Developer tab on Microsoft Excel

Now developer tab is clicked and after that macros tab is clicked. A window will open and macro1 will be automatically selected. Run tab is pressed. We have to wait until the macro1 will finish the task. After few second bin table and the power curve will be displayed.

When we want to do analyze again, we have to delete all the previous .dat files including all.dat file from C:\sugen5KW folder and we have to proceed from step a to step d.

Note that there is a limitation for data in Microsoft excel file, and analysis of the data also depends on the available resource of PC. These macros are limited to analysis up to three days data file (sampling time 1hz or higher).

A video regarding the data analysis using the macros as described above has been created.

The web link of the video is:

<http://www.youtube.com/watch?v=W2UnYamP1y>

Appendix B

Values of Simulation Block Parameters for Chapter Four

Values of simulation block parameters for chapter four are listed in Table B-1.

Table B-1: Values of simulation block parameters for chapter four

Simulation block	Parameter	Value
Wind turbine	Air density, ρ	1.225 Kg/m ³
	Blade radius, r	.9 m
	C_p _max	0.5
	λ _opt	6
Generator	Stator Phase resistance, Rs	1.6 Ω
	Inductance, Ld/Lq	0.006365 H
	Number of pole	4
Boost Converter	C1	10 μ F
	C2	10 μ F
	L1	2 mH
PWM generator	Carrier frequency	1080 Hz
	Modulation Index, m	1
	Frequency of the output voltage, f	60Hz
Transformer	Rating	1.5 KVA, 60 Hz
	Primary side voltage (p-p)	208V _{rms}
	Secondary Side voltage (p-p)	600V _{rms}
Grid	Voltage (p-p)	600V _{rms}

Appendix C

List of Research paper

In this section conference, poster and journal papers are listed which have been published or submitted to publish during this masters program. The first one is a conference papers which has been published and presented in IEEE conferences. The second one is the journal paper which has been published in “International Journal of Energy Science”. The third one is also a journal paper which has been submitted and it is under review. The fourth and fifth are poster presentations.

Paper 1: Md. Alimuzzaman, M.T. Iqbal, “Dynamic modeling and simulation of a 1kW wind turbine based water pumping system”, presented at *20th IEEE, NECEC*, 2011.

Paper 2: Md. Alimuzzaman, M.T. Iqbal, Gerald Giroux, “An Investigation of Power Performance of Small Grid Connected Wind Turbines under Variable Electrical Loads” *International Journal of Energy Science*, Vol. 2, Iss. 6, pp. 282-289, December 2012.

Paper 3: Md. Alimuzzaman, M.T. Iqbal, “Design of a Control System for Active and Reactive Power Control of a Small Grid Connected Wind Turbine” submitted for review at *International Journal of Energy Science*.

Paper 4: Md. Alimuzzaman, M.T. Iqbal. “Power performance of two small grid connected wind turbines” presented at *WESNet Student Poster Session and Competition*, October 18, 2012, Toronto, Ottawa, Canada.

Paper 5: Md. Alimuzzaman, M.T. Iqbal “Dynamic Modeling, simulation and optimization of a novel 5kW grid connected vertical axis wind turbine system” presented at *21st IEEE, NECEC, 2012.*